Electronic Supplementary Material (ESI) for Inorganic Chemistry Frontiers.
This journal is © the Partner Organisations 2023

Electronic Supporting Information

Different element substituted phosphomolybdates were synthesized in this work. Every compound was analyzed in detail using vibrational spectroscopy (infrared (IR) and Raman), ultraviolet visible (UV-Vis) spectroscopy and inductively coupled plasma optical emission spectrometry (ICP-OES). Hydration water contents (unit mol of water/mol of POM) were calculated from datasets that have been obtained using thermogravimetric analysis (TGA). Single crystals were prepared, and the structure was determined using single crystal X-ray diffraction (sc-XRD). Furthermore, powder X-ray diffractograms (p-XRD) were measured of each compound. Moreover, ^{31}P and if possible ^{51}V nuclear magnetic resonance (NMR) spectroscopy was used to characterize the compounds in solution. The Redox activity was investigated using electrochemical methods such as cyclic voltammetry (CV) and square wave voltammetry (SWV).

1 Experimental Details

1.1 Chemicals

The chemicals used in this work were obtained from the following suppliers:

- Sodium molybdate dihydrate: Carl Roth with a purity of 99.5 %
- Sodium tungstate dihydrate: VWR chemical with a purity of 99 %
- Disodium hydrogen phosphate: Merck (pro analysis)
- Sodium vanadium oxide: Alfa Aesar with a purity of 96 %
- Niobium(V) oxide: Alfa Aesar with a purity of 99.5 % (metals basis)
- Tin (grained pure): Merck (Art. 780a)
- Iron(III) chloride: Merck (anhydrous)
- Indium hydroxide: Thermo scientific with a purity of 99.8 % (metals basis)
- Cobalt(II) acetate tetrahydrate: ABCR chemical with a purity of 98 %
- Nickel(II) acetate tetrahydrate: Aldrich Chemistry with a purity of 99.0 %
- Copper(II) chloride dihydrate: Alfa Aesar with a purity of 99 %
- Zinc (grained pure): Merck
- Hydrochloric acid: VWR chemicals as 37 % solution in water
- Hydrogen peroxide: VWR chemicals as 30 % solution in water
- Potassium hydroxide: Chemsolute with a purity of 85 % (Art. 1681.1000)
- Potassium chloride: Thermoscientific with a purity of 99 %
- Sodium carbonate: Grüssing with a purity of 99.5 %
- Tetrabutylammonium bromide (TBAB): Carl Roth with a purity of 99 %
- Deuterium oxide: Deutero GmbH with a purity of 99.9 %
- Acetonitrile: VWR chemicals (HiPerSolv Chromanorm for HPLC-SUPER GRADIENT Reag. Ph. Eur., USP, ACS; water < 30 ppm – suitable for UPLC/UHPLC instruments)

Further used:

- Campingaz, mixture of butane and propane
- Deionized water was used as solvent

For some precursor compounds, stoichiometry was calculated based on mass fraction of the metal rather than nominal molar mass, to account for impurities or hydration water. The following values were used:

- Iron(III) chloride: 25.95 wt-% Fe.
- Cobalt(II) acetate dihydrate: 23.2 wt-% Co.
- Nickel(II) acetate dihydrate: 22.7 wt-% Ni.
- Copper(II) chloride: 35.65 wt-% Cu.

Potassium hexaniobate *x* hydrate: Before KNb was used for synthesis, elemental analysis was used to determine the Nb content, which is the basis for all stoichiometric calculations. The mass percentages for Nb fluctuate in the range between 37 % and 41 % depending on the crystal water content.

1.2 Analytical methods

ICP-OES:

All samples were analyzed using an ICP-OES-spectrometer for elemental analysis (Fa. Spectro, type ARCOS) for Mo, W, V, In and P (method ICP-OES). The elements Fe, Co, Ni, Cu, Zn and Sn were measured with an AAS-F (Fa. Thermo, type Solaar S Series) (method: F-AES without HKL).

- Sample preparation KNb: the initial weight was dissolved in water (1 mL), 30 % hydrogen peroxide in water (1 mL) and acidified with 37 % hydrochloric acid solution in water.
- Sample preparation $NaPV_3Mo$, $NaPIn_3Mo$, NaPCoMo, NaPNiMo and LHPA-3: the initial weight was dissolved in water (5 mL), acidified with a 65 % nitric acid solution in water (100 µL), and the solution was filled up with water to 25 mL in a volumetric flask.
- Sample preparation $NaKPV_2NbMo$, $NaKPVNb_2Mo$, NaPFeMo and NaPZnMo: the initial weight was dissolved in water (5 mL) and the solution was filled up with water to 25 mL in a volumetric flask.
- Sample preparation NaKPNbMo and $NaKPNb_3Mo$: the initial weight was dissolved in water (5 mL) and the solution was filled up with water to 25 mL in a volumetric flask.
- Sample preparation $NaKPNb_2Mo$: the initial weight was dissolved in water (5 mL), warmed up to ensure complete dissolution and the solution was filled up with water to 25 mL in a volumetric flask.

- Sample preparation NaPSnMo: the initial weight was dissolved in 96 % sulfuric acid (2 mL), 65 % nitric acid (0.5 mL), 37 % hydrochloric acid (10 mL) and the solution was filled up with 3 M hydrochloric acid solution in water to 50 mL in a volumetric flask.
- Sample preparation nBu_4NPCu_2Mo: the initial weight was dissolved in inverse aqua regia (3 HNO_3/1 HCl) (6 mL), hydrofluoric acid (1 mL) and was filled up with water to 25 mL in a volumetric flask (Anton Paar/Organic high).

TGA analysis:

TGA measurements were performed with a TG 209 F1 Libra of NETZSCH. The data were processed with the software Proteus from NETZSCH. About 20 mg of the sample was weighed into a duran-glas crucible and the change in mass was measured at the following temperature program:

- Tare
- 1 minute waiting time
- Heating to 30 °C with maximum heating rate
- Stay at 30 °C for 15 minutes
- Heating to 350 °C with a heating rate of 10 K/min
- Stay at 350 °C for 30 minute
- The sample was then cooled to room temperature

Starting temperature was below 30 °C. During all measurements, a nitrogen flow of 60 sccm/min was passed through the instrument. A measurement with an empty crucible was used for background correction. The TGA data show three regions: hygroscopic water (water that comes from the air), lattice water (water from crystal association) and the mass consistency (pure POM without any moisture). The final data were exported as a *x*/*y* text document. With the use of Origin® 2019b the TGA data were plotted as follows: on the *y*-axis the mass difference measured in mg and on the *x*-axis the temperature measured in °C.

IR spectroscopy

IR spectra were measured in attenuated total reflection (ATR) measurement mode on a QATR™-S single-reflection ATR (with a diamond prism) from Shimadzu. From the raw data obtained, the baseline was corrected, and the peaks were determined manually. The IR data were then exported as an *x*/*y* text document.

Raman spectroscopy

Raman spectra were measured on a SENTERRA Raman microscope from Bruker Optik GmbH. The aperture was set to 50 x 1000 µm. A 20 objective was used on the microscope. The excitation laser has a wavelength of 785 nm and the measurement range used was between 75 cm^{-1} and 1525 cm^{-1}. The integration time was 16 seconds, the number of scans was 8 and the Raman laser power was 10 mW.

Single crystal structures:

A description on how the crystals were obtained can be found below.

All single crystals were measured on a 4-circle single crystal diffractometer SuperNova from Oxford Diffraction (Company: Agilent Technologies, Acquisition: Nov. 2011, using a molybdenum and copper source (dual instrument), Microfocus tubes, cryostream-700 Plus nitrogen steam cooling, 100-500 K (Oxford Cryosystems)). The crystal structure data were solved and refined using Olex2 v1.5 and the ShelX algorithm, as well as the PLATON software.[1–5] In some cases, Shelxtl XPREP tool was used for space group determination. Some details on the refinement of the individual crystal structure data sets in Olex2 v1.5 are explained below:

- The crystals were obtained by slow evaporation of water on air. Dataset for LHPA-3 was solved using ShelXS, direct methods and refined using ShelXL (L. S.). The space group is $P6_3$ (173). Hydrogen atoms of the hydration water molecules were not modeled due to the low scattering contribution. A solvent mask (SQUEEZE) was used (1.167 molecules water). R_1: 1.85 %, wR_2: 5.38 %, R_{int}: 3.28 % and Goof: 1.098. The .cif file is available in the CCDC data base with the deposition number 2205006.
- The crystals were obtained by crystallizing from an aqueous concentrated solution. Dataset for KNb was solved using ShelXS, direct methods and refined using ShelXL (L. S.). The space group is $P2_1/c$ (14) (space group determination Shelxtl XPREP). Hydrogen atoms of the hydration water molecules were not modeled due to the low scattering contribution. R_1: 2.58 %, wR_2: 6.73 %, R_{int}: 3.08 % and Goof: 1.252. The .cif file is available in the CCDC data base with the deposition number 2216947.
- The crystals were obtained by slow evaporation of water under reduced pressure in a desiccator. Dataset $NaPV_3Mo$ was solved using ShelXS, direct methods and refined using ShelXL (L. S.). The space group is $P\text{-}42_1c$ (114) (space group determination Shelxtl XPREP). The crystal structure dataset is a twinned structure with an inversion twin (Flack

parameter ~0.5). So, the following twin law was used: -1 0 0 0 -1 0 0 0 -1 (BASF 0.5). Hydrogen atoms of the hydration water molecules were not modeled due to the low scattering contribution. R_1: 3.03 %, wR_2: 7.84 %, R_{int}: 4.49 % and Goof: 1.089. The .cif file is available in the CCDC data base with the deposition number 2205007.

- The crystals were obtained by slow evaporation of water on air. Dataset $[P_2Mo_{18}O_{62}]^{6-}$ was solved and refined using ShelXT, intrinsic phasing. The space group is *P-1* (2). Hydrogen atoms of the hydration water molecules were not modeled due to the low scattering contribution. A solvent mask (SQUEEZE) did not improve the model. R_1: 3.83 %, wR_2: 10.07 %, R_{int}: 2.98 % and Goof: 1.030. The .cif file is available in the CCDC data base with the deposition number 2216946.

Powder XRD:

Powder XRD diffractograms were measured on an X'Pert Pro diffractometer (Panalytical MPD Corp.) using Cu-K_α radiation (λ = 1.5418 Å) in the range of 5-90 ° (step size 0.013 °, counting time 73 seconds) using a PIXcel-Detektor (256 canals with the angle range 3.12 ° 2θ). For this purpose, the background was determined, and the data smoothed. The reflexes were then determined.

NMR spectroscopy

All NMR spectra were measured with a Bruker AVANCEII 600 MHz. The samples were prepared as follows: The respective POM (70 mg) was dissolved in deionized water (0.63 mL), which had previously been adjusted to pH 1 with a 2 M hydrochloric acid solution in deionized water, and D_2O (0.07 mL) was added. Sample nBu_4NPCu_2Mo was measured only in acetone-*d*6. All ^{31}P spectra were measured with a Time Domain Data Sizes (TD) of 32 K, the Number of Scans (NS) were set to 2k (= 2048), the Transmitter Frequency Offset for Channel F1 (O1) and the Spectral Width (SW) were -1 and 40 ppm. The Delay D1 was set to 1 s. For the ^{51}V experiments TD was 32 K, O1 and SW -520 and 400 ppm, D1 0.5 s and NS was set to 4 K. ^{119}Sn-NMR experiment was done using tetramethyl tin in benzene-*d*6 as external standard. The NMR analyses were carried out with the software MestReNova®. In MestReNova®, the peaks were first determined, and the data subsequently exported in .csv format.

UV-Vis spectroscopy

The UV-Vis spectra were measured with a Cary 60 UV-Vis spectrometer (Agilent Technologies) in a 3 mL Quartz cuvette (QS). The measurements were carried out using the Cary WinUV software. Measurements were taken in the measuring range between 200 nm and

800 nm. The absorption was measured in the slow measurement mode. The data were then exported as a csv data set. All samples were prepared as follows: The POMs (10 mg) were dissolved in water (10 mL) and the resulting solution was diluted in a cuvette with a total volume of 3 mL to corresponding 3 mL solution volume (usually make up 0.01 mL of stock solution to 3 mL water in the cuvette). Sample nBu_4NPCu_2Mo was handled analogue but the solvent was acetonitrile.

Electrochemistry (CV and SWV):

The CV/SWV measurements were carried out in aqueous, hydrochloric acid medium at pH 1 and a concentration of 1 mmol/L on a Metrohm - Autolab PGSTAT101. For nBu_4NPCu_2Mo the solvent was acetonitrile and to the solution tetrabutylammonium hexafluorophosphate was added as a conducting salt. During the measurement, the solution was purged with nitrogen. The working electrode was a glassy carbon electrode (diameter: 3 mm), the reference electrode was the Ag/Ag^+ electrode. The counter electrode was a platinum electrode. Measurements were taken in the measuring range between -0.6 and 1 V with a scan rate (for CV) of 100 mV/s for 3 scans. All SWV measurements were taken with a scan rate of 5 mV/s, a modulation amplitude of 20 mV and a frequency of 25 Hz. The measurements were carried out with the software Ivium and the data was subsequently exported as an *x*/*y* text document.

Other:

The exported *x*/*y* data were then imported into Origin® 2019b and plotted as corresponding graphs. All graphs in this paper were thus created in Origin®.

1.3 Synthesis of $Na_9[PMo_9O_{34}]$

Sodium molybdate dihydrate (9.7027 g, 40.10 mmol, 6.95 equivalents) and disodium hydrogen phosphate (0.8186 g, 5.766 mmol, 1 equivalent) were dissolved in water (50 mL). The pH of the colorless solution was 8.987 and was adjusted to 1.035 with a 37% hydrochloric acid solution in water, turning the solution yellow. The mixture was evaporated on air, yielding a yellow solid as well as single crystals for X-ray diffraction. A yellow solid (3 g) was obtained, which still contains a significant amount of NaCl.

Characterization:

^{31}P-NMR (242.9 MHz, H_2O/acetone-*d*6, 20 °C): δ [ppm] = -0.232 (broad, **P**O_4^{3-}), -3.10 (s, LHPA-3), -3.73 (s, H**P**Mo).

IR (ATR): $\tilde{\nu}$ [cm^{-1}] = 3379 (w, O-H, H_2O), 1613 (O-H, hydration H_2O), 1059, 1008 (me, P-O), 961, 937, 925, 904 (me, M=O_t), 849 (me, (M-O-M)$_{vertex}$), 767, 698 (st, (M-O-M)$_{edge}$).

UV-Vis [nm]: 215, 317.

ICP-OES: Calculated for $Na_9[PMo_9O_{34}] \cdot 6\ H_2O$: 49.245 % Mo, 1.766 % P, 11.8 % Na, 0 % K. Found for $Na_9[PMo_9O_{34}] \cdot 6\ H_2O$: 32.5 % Mo, 1.40 % P, 18.0 % Na, 0 % K. Data normalised to molybdenum. P/Mo/Na/K ratio: 1.2/9/20.8/0.

This compound is not pure. There is an excess of NaCl impurities.

TGA: 6.180 % weight loss upon drying, this corresponds to 6 mol lattice water per mol of the POM.

The crystals were obtained using the slow evaporation method on air.

1.4 Synthesis of $K_8[Nb_6O_{19}]$

Diniobiumpentoxide (22.6273 g, 85.13 mmol, 1 equivalent) and potassium hydroxide (71.0398 g, 1.27 mol, 14.87 equivalents) were mixed and the mixture was added in portions to a nickel crucible heated over a gas burner flame (Campingaz, mixture butane/propane). The reaction mixture began to bubble due to carbon dioxide formation and water evaporation. The diniobiumpentoxide began to dissolve in the potassium hydroxide melt. After the addition was completed, the reaction mixture was heated further until the bubbling stopped and the melt became viscous. It was cooled to room temperature and water was added to the solidified, hard, gray melt and heat evolution was observed. To dissolve the melt, it was first mechanically crushed in the crucible. The colorless solution was filtered and the crucible rinsed several times. Subsequently, the volume of the filtrate was reduced to one-eighth under reduced pressure, resulting in precipitation of a colorless solid. The supernatant turned brownish. It was cooled to 4 °C overnight. The precipitate was filtered and washed several times with ethanol cooled to 4 °C. This was followed by drying at 60 °C. A colorless solid (25.2479 g) was obtained.

Characterization:

IR (ATR): $\tilde{\nu}$ [cm^{-1}] = 2950 (w, O-H, H_2O), 1636 (O-H, hydration H_2O), 1551, 1453, 1374 (w, CO_3^{2-}), 849, 829 (me, M=O_t), 656 (st, (M-O-M)$_{asym.}$), 512 (st, (M-O-M)$_{sym.}$).

UV-Vis [nm]: 247.

ICP-OES: Calculated for $K_8[Nb_6O_{19}] \cdot 5\ H_2O$: 44.091 % Nb, 24.74 % K, 0 % Na. Found for $K_8[Nb_6O_{19}] \cdot 5\ H_2O$: 40.92 % Nb, 24.8 % K, 0.09 % Na. Data normalised to niobium. K/Na/Nb ratio: 8.64/0.053/6.

TGA: 7.369 % weight loss upon drying, this corresponds to 5 mol lattice water per mol of the POM.

The crystals were obtained by slow evaporation of an aqueous solution under ambient conditions.

Synthesis of $K_8[Nb_6O_{19}]$ (KNb) was adapted from the literature procedure.[6,7] Elemental analysis and TGA results summarized in Table 1:

Table 1: Results from ICP-OES and TGA analysis of KNb.

Compound	Molecular composition	K/Na/Nb ratio[a]	Hydration water [b] [mol/mol-POM]
KNb	$K_8[Nb_6O_{19}]$	8.64/0.0533/6	5

KNb is $K_8[Nb_6O_{19}]$

[a]The ratio K/Na/Nb were determined by AAS/ICP-OES analysis. The data were normalized to the target Nb content. There is a little bit more K than expected, due to the carbonates that are forming while heating a melted KOH solution.

[b]The content of hydration water was determined by TGA analysis.

Data are normalized to the target Nb content. There is more K than expected for KNb. During heating a melted KOH solution, the KOH reacts with carbon dioxide from air to form potassium carbonate.[8] Normally carbonate decomposes at these temperatures, but apparently carbonate is also formed during the cooling phase that remains stable after cooling. Hydration water content was determined to be five molecules water per POM molecule using TGA.

Figure S1 shows an ATR-FT-IR spectrum from KNb with the characteristic vibrational bands.

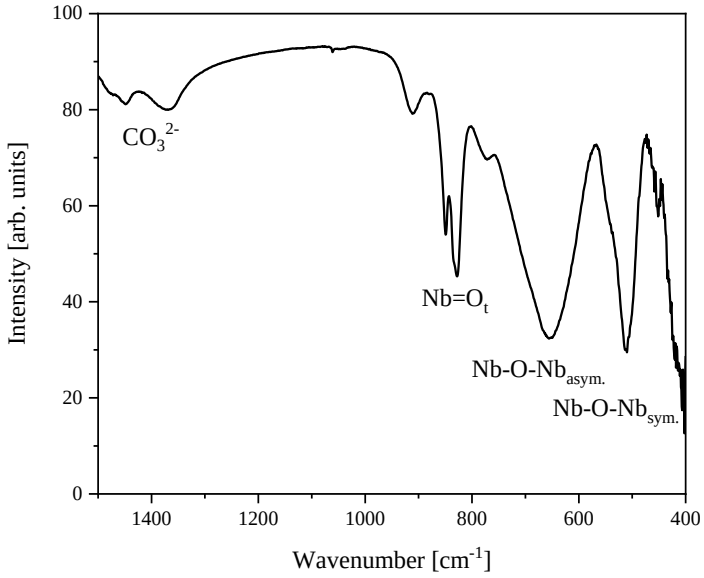

Figure S1: FT-IR data of KNb. Vibration band of terminal oxygen-metal Nb=O_t (849 cm^{-1} and 828 cm^{-1}) and asymmetric and symmetric vibration of Nb-O-Nb (656 cm^{-1} and 510 cm^{-1}).

The FT-IR data in Figure S1 verify the integrity of the Lindqvist structure-type for KNb. Around 1400 cm^{-1} there is the vibration band from carbonate visible that is forming during the synthesis of KNb.[9] There are the following vibration bands: two vibration bands for the vibration of the terminal oxygen metal bond M=O_t at 849 cm^{-1} and 828 cm^{-1} and one asymmetric and one symmetric Nb-O-Nb band at 656 cm^{-1} and 510 cm^{-1}.[10,11]

In the Raman spectrum in Figure S2 the vibration bands between 800 cm^{-1} and 1000 cm^{-1} belong to the symmetric (884 cm^{-1}) and asymmetric (828 cm^{-1}) vibration of the Nb=O_t bond. The vibration band at 462 cm^{-1} and 539 cm^{-1} can be assigned to the symmetric Nb-O-Nb vibration mode and the bands under 400 cm^{-1} are vibration modes from the asymmetric Nb-O-Nb bonds.[10]

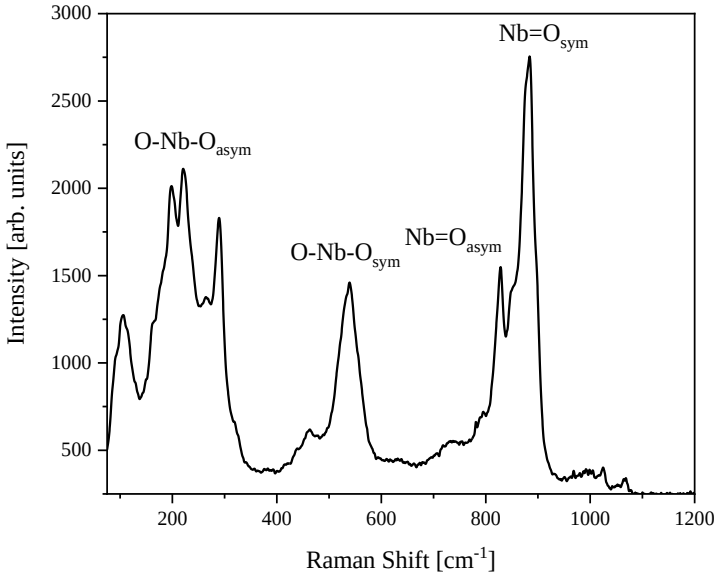

Figure S2: Raman data of KNb. Vibration of terminal oxygen-metal bonds Nb=O_t (884 cm^{-1} and 828 cm^{-1}) and asymmetric and symmetric vibration of Nb-O-Nb (656 cm^{-1} and 510 cm^{-1}).

An UV-Vis spectrum of KNb measured in an aqueous potassium hydroxide solution is shown in Figure S3:

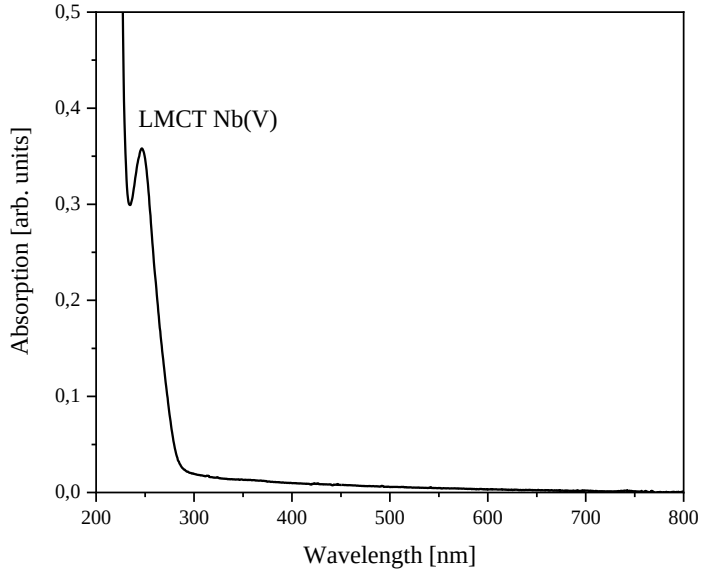

Figure S3: UV-Vis data of KNb in aqueous potassium hydroxide solution.

The LMCT O → Nb(V)O_6 was found at 247 nm.

The CV and SWV data in Figure S4 and S5 for KNb in aqueous potassium hydroxide solution.

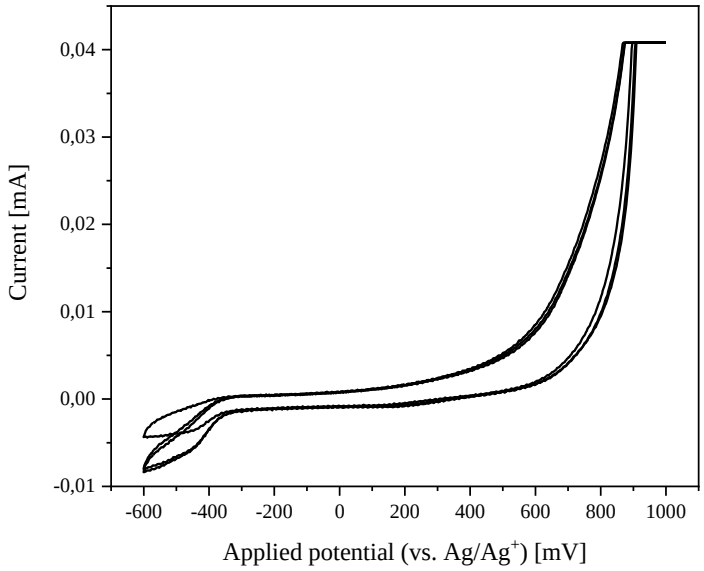

Figure S4: CV measurements of KNb in aqueous potassium hydroxide solution (concentration 1 mmol/L, scan rate 100 mV/s (CV)). Potassium hydroxide was used as conducting salt.

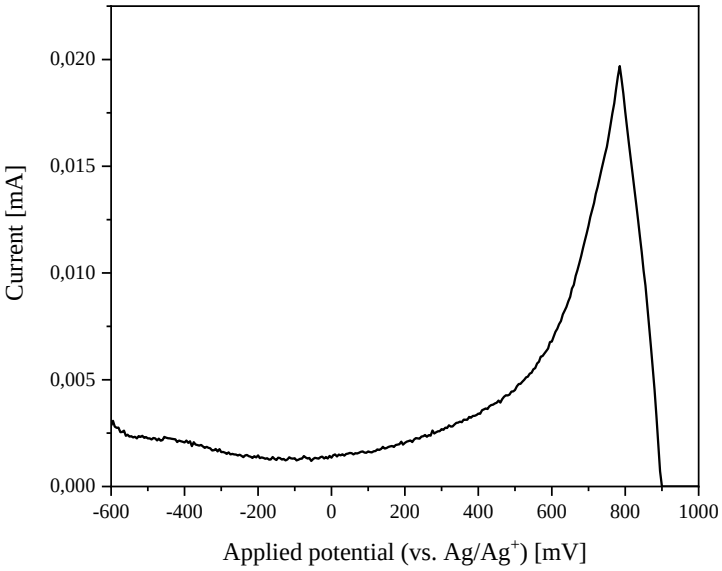

Figure S5: SWV measurements of KNb in aqueous potassium hydroxide solution (concentration 1 mmol/L, scan rate 5 mV/s (SWV)). Potassium hydroxide was used as conducting salt.

Synthesis of KNb (Figure S6):

Figure S6: Molten mixture over a gas flame of potassium hydroxide and niobium pentoxide for synthesizing KNb. A nickel crucible is used (left). Cooled melt of KNb and potassium hydroxide after KNb synthesis. A nickel crucible is used (right).

1.5 Nanofiltration

For purification, four cycles of nanofiltration were conducted. For this purpose, the start volume of the reaction solution (feed) was always 100 mL. The pressure in the system was set to 33 bar, a flow was set to 15 mL/min and the emergency shutdown pressure was set to 34 bar. In the first step, 5 mL of the feed solution was taken for analysis. The process was then started by flowing the feed solution through the system for 15 min under process conditions, where the permeate flow was recombined with the retentate flow. After this period, the permeate flow was separated from the retentate and collected. In the first cycle, 65 mL of permeate was collected and the concentrated retentate solution was diluted with 70 mL of water. In the second cycle, 70 mL of permeate was collected and the concentrated retentate solution was diluted again with 70 mL of water. A total of four cycles were performed in this manner.

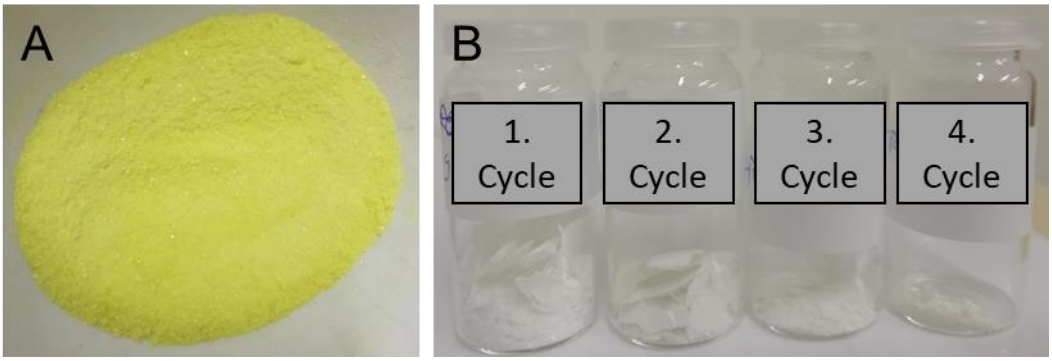

Figure S7: Visual comparison of a) intensely yellow product and b) salt fractions, both obtained by concentrating the retentate and permeate, respectively, over a rotary evaporator.

Subsequently, 5 mL of the retentate and permeate fractions were separated and used for further analysis by ICP-OES and AAS. Both the permeate and retentate fractions were dried under reduced pressure.

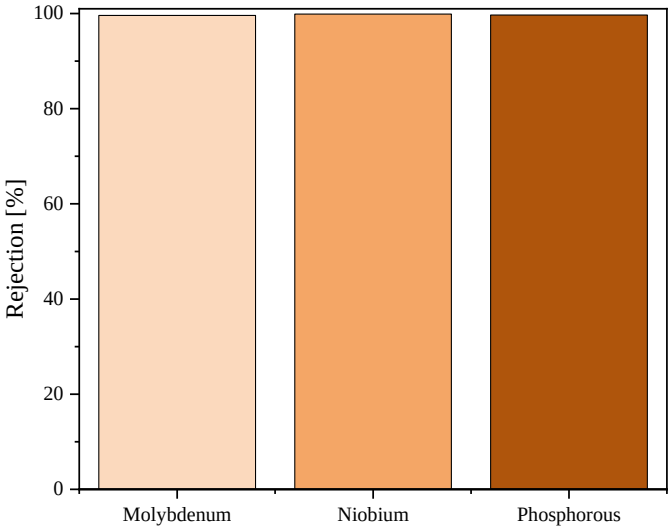

Figure S8: Rejection of the catalyst compounds Mo(VI), Nb(V) and P(V) for the $[PNb_3Mo_9O_{40}]^{6-}$ anion in our investigated nanofiltration membrane process.

The powder XRD data of the dried permeate fractions (Figure S9) all show reflexes belonging to NaCl.

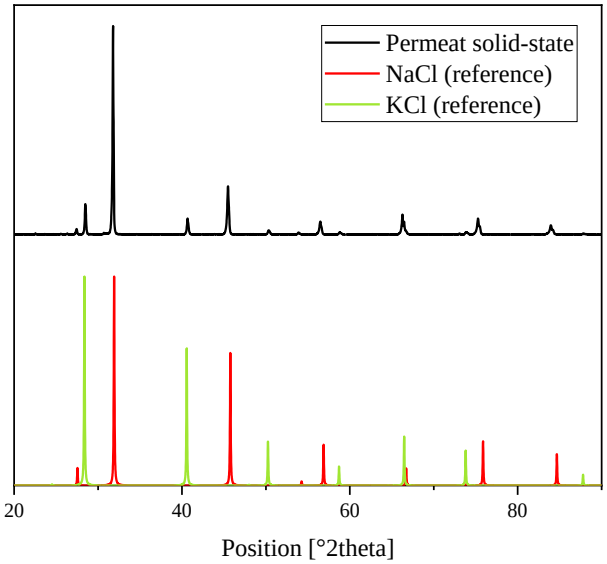

Figure S9: Comparison of the powder XRD diffractogram of the permeate fraction of the purification experiment of $NaKPNb_3Mo$ with NaCl (ICSD: 142801) and KCl (ICSD: 165593). To get a better view all data were normalized.[12,13]

Furthermore, there are low intensity reflexes that can be assigned to KCl.[12,13] Thus, the permeate fraction can be identified without doubt as a mixture of NaCl and KCl, which was to be shown.

1.6 Synthesis of the transition metal substituted POMs using LHPA-3

In general the idea for the synthesis of the transition metal substituted POMs based on the following concept: the lacunary LHPA-3 was prepared *in situ* and the foreign metal precursor compound(s) were added in the right stoichiometry. If necessary, sodium molybdate dihydrate was added to fill the remaining vacancies of the lacunary compound. The reaction mixture was heated to reflux for 30-60 minutes and then cooled to room temperature. After cooling the pH value was measured and if necessary corrected to ~1 by adding a 37 % solution of hydrochloric acid in water. The reaction mixture was filtered and desalinated using our newly presented nanofiltration process.

1.6.1 In situ Lacunary synthesis

Sodium molybdate dihydrate and disodium hydrogen phosphate were dissolved in water. The pH of the colorless solution was ~8.7 and was adjusted to ~1 with a 37 % hydrochloric acid solution in water, turning the solution yellow.

Table 2 shows an overview of the precise weights of the precursor compounds for the respective POMs:

Table 2: Weights of all precursor compounds for *in situ* synthesis of LHPA-3 for each experiment.

POM	Sodium molybdate dihydrate [g]	Disodium hydrogen phosphate [g]	Volume of water [mL]
NaPCoMo	10.0058	0.6535	50
NaPNiMo	10.0000	0.6540	50
nBu_4NPCu_2Mo	10.0064	0.6545	50
NaPZnMo	8.1400	0.5333	50
NaPFeMo	10.0024	0.6544	50
NaPIn_3Mo	10.0056	0.6538	50
NaPSnMo	10.2486	0.6692	50
NaPNbMo	10.0069	0.6537	50
NaPNb_2Mo	10.0005	0.6532	50
NaPNb_3Mo	10.0063	0.6561	50
NaPV_2NbMo	15.0041	0.9801	50
NaPVNb_2Mo	10.0021	0.6528	50
NaPV_3Mo	10.0029	0.6570	50

$NaPW_3Mo$	10.0028	0.6573	50

1.6.2 Synthesis of Co(II), Ni(II), Cu(II), Fe(III), V(V) and W(VI) substituted POMs

For Co(II), Ni(II), Cu(II), Fe(III), V(V) and W(VI) substitution the corresponding precursor compound was added in the right stoichiometry to the *in situ* formed LHPA-3 lacunary species. Then sodium molybdate dihydrate was added to fill the remaining vacancies of LHPA-3 and the solution was heated to reflux for 30 min. After this procedure the solution was cooled to room temperature and the pH value was measured. If necessary, the pH value was adjusted to ~1 by adding a 37 % solution of hydrochloric acid in water. In the next step the mixture was filtered and purified using the dialysis nanofiltration process.

Table 3 summarizes all amounts for the corresponding precursor compounds and the pH values used for the synthesis. For some metal precursor compounds it was necessary to first determine the metal content by elemental analysis, since some preliminary experiments showed that the precursor compounds apparently contain more hydration water than indicated by the supplier. With the help of the determined metal content, it was then possible to calculate a more accurate weight for the respective precursor compound, based on the foreign metal.

Table 3: Weights of the precursor compounds/pH values used for the experiments to synthesize Co(II), Ni(II), Cu(II), Fe(III) and V(V) substituted POMs.

POM	Foreign metal precursor [g]	Equivalents	Sodium molybdate dihydrate [g]	Equivalents	pH value after addition	pH value corrected
NaPCoMo	1.3648 (cobalt(II) acetate tetrahydrate)	1 (aacording to Co(II))	2.2233	2	4.888	1.496
NaPNiMo	1.1875 (nickel(II) acetate tetrahydrate)	1	2.2222	2	4.498	1.646
$nBu4NPCu_2Mo$	1.8917 (copper(II) chloride)	2.3 (according to Cu(II))	1.1123	1	1.664	-
NaPFeMo	0.9872 (iron(III) chloride)	1 (according to Fe(III))	2.2228	2	1.910	-

$NaPV_3Mo$	1.6808 (sodium vanadate)	3	-	-	4.420	-
$NaPW_3Mo$	4.5450 (sodium tungstate dihydrate)	3	-	-	8.701	1.858

For product isolation of nBu_4NPCu_2Mo the compound was precipitated by adding a colorless solution of tetrabutylammonium bromide (17.7826 g, 55.16 mmol, 11.96 equivalents) in water (30 mL) to the green reaction solution. A green precipitate was formed which was collected by filtering and was washed several times using water. The green solid was dried using a desiccator over orange yellow. During this time the color changed from green to brown.

1.6.3 Synthesis of the In(III) substituted POM

For compound $NaPIn_3Mo$ the In(III) precursor was treated as follows:

Indium(III) hydroxide (2.2859 g, 13.78 mmol, 3.00 equivalents) was dissolved in a 37 % hydrochloric acid solution in water (10 mL). A clear, colorless solution was formed.

The In(III) solution was added to the LHPA-3 solution, refluxed for 30 min and was than cooled to room temperature. The pH value was -0.566 and was adjusted to 1.947 using a 1 M sodium carbonate solution in water. In the next step the mixture was filtered and purified using the dialysis nanofiltration process.

1.6.4 Synthesis of Zn(II) and Sn(IV) substituted POMs

The precursor compounds for the experiments to synthesize Zn(II) and Sn(IV) substituted POMs were the corresponding elements Zn and Sn.

Grained zinc (0.2445 g, 3.738 mmol, 1.00 equivalent) was dissolved in a 37 % hydrochloric acid solution in water (10 mL). A gas formation and bubbling was visible and the mixture became hot. A clear, colorless solution was formed.

Tin granules (0.5587 g, 4.706 mmol, 1.00 equivalent) were dissolved in a 37 % hydrochloric acid solution in water (22 mL). A gas formation was visible and the mixture became warm. For complete dissolution of tin, the mixture was heated to 100 °C until everything was dissolved. A clear, colorless solution was formed.

After addition of the Sn(II) solution to the LHPA-3 solution, the solution turned into dark. A 30 % solution of hydrogen peroxide in water (12 mL) was added to oxidize Sn(II) to Sn(IV). The mixture was than heated to reflux for 60 min. During this time the color of the reaction mixture turned from dark to yellow and was than cooled to room temperature. In the next step the reaction mixture was extracted three times using diethyl ether (30 mL). During the extraction process a third phase formed and sat down. The collected and united POM ether phases were concentrated under reduced pressure to yield a yellow solid.

1.6.5 Synthesis of Nb(V) and Nb(V)/V(V) mixed substituted POMs

The V(V) free, only Nb(V) substituted POMs were prepared as follows:

Potassium hexaniobate was dissolved in a 1.5 % hydrogen peroxide solution in water (20 mL) and was directly added to the LHPA-3 reaction solution. The mixture gets than refluxed. In some cases, after potassium hexaniobate addition a clear, orange colored solution is forming or a solid is precipitating. This is not always a problem when the solution is heated up fast enough. Then a clear orange solution is formed and sodium molybdate dihydrate is added. After the addition of sodium molybdate dihydrate the color turned into yellow again. The solution was heated to reflux for 60 min and was than cooled to room temperature. The pH value was adjusted to ~1.6 using a 37 % hydrochloric acid solution in water. In the next step the mixture was filtered and purified using the dialysis nanofiltration process.

V(V) and Nb(V) mixed substituted POMs were prepared as follows:

Potassium hexaniobate was dissolved in a 1.5 % hydrogen peroxide solution in water (20 mL) and was directly added to the reaction solution. The mixture gets than refluxed. In some cases after potassium hexaniobate addition a clear, orange colored solution is forming or a solid is precipitating. This is not always a problem when the solution gets fast enough heated up. Then a clear orange colored solution gets formed. In the next step sodium vanadate was added and a clear, red colored solution was formed. The solution was heated to reflux for 30 min and was than cooled to room temperature. The pH value was adjusted to ~1.6 by adding a 37 % hydrochloric acid solution in water. In the next step the mixture was filtered and purified using the dialysis nanofiltration process.

Table 4 summarizes the amounts of the foreign metal precursors used for synthesizing the Nb(V) and Nb(V)/V(V) mixed substituted POMs. Since different batches of potassium hexaniobate contain different amounts of hydration water, from every bath the Nb(V)

content was determined using elemental analysis. From this value the exact weights were calculated:

Table 4: Weights of the precursor compounds/pH values used for the experiments to synthesize Nb(V) and Nb(V)/V(V) mixed substituted POMs.

POM	KNb [g]	Equivalents according to Nb(V)	Sodium vanadate/Sodium molybdate tetrahydrate [g]	Equivalents	pH value after addition	pH value corrected
NaKPNbMo	1.1216	1	2.2241 (molybdate)	2	5.142	1.604
$NaKPNb_2Mo$	2.1642	2	1.1118 (molybdate)	1	4.789	1.322
$NaKPNb_3Mo$	3.3621	3	-	-	5.450	1.690
$NaKPV_2NbMo$	1.8222	1	1.6815 (vanadate)	2	5.351	-
$NaKPVNb_2Mo$	2.1632	2	0.5598 (vanadate)		5.235	1.858

1.7 Characterization

NaPCoMo:

^{31}P-NMR (242.9 MHz, H_2O/D_2O, 20 °C): δ [ppm] = -0.54, -1.77, -3.36.

IR (ATR): $\tilde{\nu}$ [cm^{-1}] = 3505 (w, O-H, H_2O), 1618 (O-H, hydration H_2O), 1049 (w, P-O), 946 (me, $M=O_t$), 869 (me, $(M\text{-}O\text{-}M)_{vertex}$), 772, 707 (st, $(M\text{-}O\text{-}M)_{edge}$).

UV-Vis [nm]: 210.

ICP-OES: Calculated for $Na_7[PCoMo_{11}O_{40}] \cdot 8\ H_2O$: 50.488 % Mo, 2.819 % Co, 1.482 % P, 0 % K, 7.699 % Na. Found for $Na_7[PCoMo_{11}O_{40}] \cdot 8\ H_2O$: 51.90 % Mo, 2.77 % Co, 1.54 % P 0.01 % K, 3.97 % Na. Data normalized to molybdenum. Na/K/P/Co/Mo ratio: 3.51/0.005/1.01/0.956/11.

TGA: 6.882 % weight loss upon drying, this corresponds to 8 mol lattice water per mol of the POM.

Additional protocol for the nanofiltration process:

- Cycle 1: 65 mL permeate in 29 min

- Cycle 2: 70 mL permeate in 54 min
- Cycle 3: 70 mL permeate in 77 min
- Cycle 4: 70 mL permeate in 98 min

NaPNiMo:

^{31}P-NMR (242.9 MHz, H_2O/D_2O, 20 °C): δ [ppm] = -0.42, -1.68, -3.22, -3.90.

IR (ATR): $\tilde{\nu}$ [cm^{-1}] = 3454 (w, O-H, H_2O), 1610 (O-H, hydration H_2O), 1047 (w, P-O), 942 (me, M=O_t), 869 (me, (M-O-M)$_{vertex}$), 783 (st, (M-O-M)$_{edge}$).

UV-Vis [nm]: 210.

ICP-OES: Calculated for $Na_7[PNiMo_{11}O_{40}] \cdot 8\ H_2O$: 50.494 % Mo, 2.808 % Ni, 1.482 % P, 0 % K, 7.7 % Na. Found for $Na_7[PNiMo_{11}O_{40}] \cdot 8\ H_2O$: 52.58 % Mo, 2.58 % Ni, 1.62 % P 0.00 % K, 4.58 % Na. Data normalized to molybdenum. Na/K/P/Ni/Mo ratio: 3.99/0.00/1.05/0.881/11.

TGA: 10.27 % weight loss upon drying, this corresponds to 12 mol lattice water per mol of the POM.

- Cycle 1: 65 mL permeate in 36 min
- Cycle 2: 70 mL permeate in 62 min
- Cycle 3: 70 mL permeate in 87 min
- Cycle 4: 70 mL permeate in 110 min

nBu_4NPCu_2Mo:

^{31}P-NMR (242.9 MHz, acetone-*d*6, 20 °C): δ [ppm] = -3.02, -3.60.

IR (ATR): $\tilde{\nu}$ [cm^{-1}] = 3421 (w, O-H, H_2O), 2960, 2936, 2874 (w, CH_3-/-CH_2-valence vibration), 1636 (w, O-H, hydration H_2O), 1482, 1460 (w, CH_3-/-CH_2-deformation vibration), 1380 (w, CH_3-deformation vibration), 1053 (w, -C-N valence vibration), 1077, 1055 (w, P-O), 935 (me, M=O_t), 864 (me, (M-O-M)$_{vertex}$), 777 (st, (M-O-M)$_{edge}$).

UV-Vis [nm]: 214, 306.

ICP-OES: Calculated for $(nBu_4N)_{11}[PCu_2Mo_{10}O_{40}]$: 21.684 % Mo, 2.872 % Cu, 0.700 % P, 0 % K, 0 % Na. Found for $(nBu_4N)_{11}[PCu_2Mo_{10}O_{40}]$: 34.37 % Mo, 1.85 % Cu, 1.24 % P 0 % K, 1.83 % Na. Data normalized to molybdenum. Na/K/P/Cu/Mo ratio: 2.22/0/1.11/0.813/10.

The incorporation of Cu(II) is not complete.

NaPZnMo:

^{31}P-NMR (242.9 MHz, H_2O/D_2O, 20 °C): δ [ppm] = -0.53, -0.79, -1.59, -1.66, -1.90, -2.45, -3.15, -3.27, -3.41, -3.90.

IR (ATR): $\tilde{\nu}$ [cm^{-1}] = 3515 (w, O-H, H_2O), 1620 (O-H, hydration H_2O), 1075, 1060 1045 (w, P-O), 939 (me, M=O_t), 900 (me, (M-O-M)$_{vertex}$), 775 (st, (M-O-M)$_{edge}$).

UV-Vis [nm]: 210, 311.

ICP-OES: Calculated for $Na_7[PZnMo_{11}O_{40}] \cdot 8\ H_2O$: 50.332 % Mo, 3.12 % Zn, 1.477 % P, 0 % K, 7.675 % Na. Found for $Na_7[PZnMo_{11}O_{40}] \cdot 8\ H_2O$: 51.88 % Mo, 1.21 % Zn, 1.6 % P 0.00 % K, 4.12 % Na. Data normalized to molybdenum. Na/K/P/Zn/Mo ratio: 3.65/0/1.06/0.377/11.

The incorporation of Zn(II) is not complete.

TGA: 6.993 % weight loss upon drying, this corresponds to 8 mol lattice water per mol of the POM.

Additional protocol for the nanofiltration process:

- Cycle 1: 65 mL permeate in 26 min
- Cycle 2: 70 mL permeate in 47 min
- Cycle 3: 70 mL permeate in 65 min
- Cycle 4: 70 mL permeate in 82 min

NaPFeMo:

^{31}P-NMR (242.9 MHz, H_2O/D_2O, 20 °C): δ [ppm] = no signal observed.

IR (ATR): $\tilde{\nu}$ [cm^{-1}] = 3423 (w, O-H, H_2O), 1613 (O-H, hydration H_2O), 1051 (w, P-O), 945 (me, M=O_t), 864 (me, (M-O-M)$_{vertex}$), 767 (st, (M-O-M)$_{edge}$).

UV-Vis [nm]: 211, 305.

ICP-OES: Calculated for $Na_6[PFeMo_{11}O_{40}] \cdot 8\ H_2O$: 51.126 % Mo, 2.705 % Fe, 1.501 % P, 0.00 % K, 6.682 % Na. Found for $Na_6[PFeMo_{11}O_{40}] \cdot 8\ H_2O$: 51.3 % Mo, 3.10 % Fe, 1.60 % P 0.01 % K, 3.96 % Na. Data normalized to molybdenum. Na/K/P/Fe/Mo ratio: 3.54/0.0053/1.06/1.14/9

TGA: 7.085 % weight loss upon drying, this corresponds to 8 mol lattice water per mol of the POM.

Additional protocol for the nanofiltration process:

- Cycle 1: 65 mL permeate in 23 min
- Cycle 2: 70 mL permeate in 45 min
- Cycle 3: 70 mL permeate in 66 min
- Cycle 4: 70 mL permeate in 90 min

$NaPIn_3Mo$:

^{31}P-NMR (242.9 MHz, H_2O/D_2O, 20 °C): δ [ppm] = -0.56, -1.72, -2.31, -3.19, -3.93.

IR (ATR): $\tilde{\nu}$ [cm^{-1}] = 3344 (w, O-H, H_2O), 1611 (O-H, hydration H_2O), 1058 (w, P-O), 956 (me, $M{=}O_t$), 867 (me, $(M\text{-}O\text{-}M)_{vertex}$), 770 (st, $(M\text{-}O\text{-}M)_{edge}$).

UV-Vis [nm]: 211.

ICP-OES: Calculated for $Na_{12}[PIn_3Mo_9O_{40}] \cdot 20\ H_2O$: 34.332 % Mo, 13.696 % In, 1.232 % P, 0.00 % K, 10.969 % Na. Found for $Na_{12}[PIn_3Mo_9O_{40}] \cdot 20\ H_2O$: 41.35 % Mo, 13.91 % In, 1.48 % P 0.00 % K, 1.78 % Na. Data normalized to molybdenum. Na/K/P/In/Mo ratio: 1.62/0/1/2.53/9.

The incorporation of In(III) is not complete.

TGA: 14.37 % weight loss upon drying, this corresponds to 20 mol lattice water per mol of the POM.

Additional protocol for the nanofiltration process:

- Cycle 1: 65 mL permeate in 46 min

- Cycle 2: 70 mL permeate in 81 min
- Cycle 3: 70 mL permeate in 110 min
- Cycle 4: 70 mL permeate in 138 min

NaPSnMo:

This compound was identified to be HPMo using only NMR- FT-IR and the calculated ICP-OES data.

^{31}P-NMR (242.9 MHz, H_2O/D_2O, 20 °C): δ [ppm] = -3.90.

IR (ATR): $\tilde{\nu}$ [cm^{-1}] = 3507 (w, O-H, H_2O), 1604 (O-H, hydration H_2O), 1058 (w, P-O), 957 (me, M=O_t), 879 (me, (M-O-M)$_{vertex}$), 744 (st, (M-O-M)$_{edge}$).

ICP-OES: Calculated for $Na_5[PSnMo_{11}O_{40}] \cdot 9\ H_2O$: 49.731 % Mo, 5.594 % Sn, 1.460 % P, 0.00 % K, 5.417 % Na. Found for $Na_5[PSnMo_{11}O_{40}] \cdot 9\ H_2O$: 56.97 % Mo, 0.00 % Sn, 1.69 % P 0.00 % K, 0.07 % Na. Data normalized to molybdenum. Na/K/P/Sn/Mo ratio: 0.0571/0/1.01/0/11. Calculated for $H_3[PMo_{12}O_{40}] \cdot 9\ H_2O$: 57.929 % Mo, 1.559 % P, 0.00 % K, 0.00 % Na.

TGA: 7.817 % weight loss upon drying, this corresponds to 9 mol lattice water per mol of the POM.

NaPNbMo:

^{31}P-NMR (242.9 MHz, H_2O/D_2O, 20 °C): δ [ppm] = -1.28, -1.37, -1.43, -2.99, -3.29, -3.30, -3.36, -3.38, -3.66

IR (ATR): $\tilde{\nu}$ [cm^{-1}] = 3396 (w, O-H, H_2O), 1615 (O-H, hydration H_2O), 1058, 1034 (w, P-O), 944 (me, M=O_t), 859 (me, (M-O-M)$_{vertex}$), 741 (st, (M-O-M)$_{edge}$).

UV-Vis [nm]: 209, 301.

ICP-OES: Calculated for $Na_4[PNbMo_{11}O_{40}] \cdot 6\ H_2O$: 52.264 % Mo, 4.601 % Nb, 1.534 % P, 0.00 % K, 4.554 % Na. Found for $Na_4[PNbMo_{11}O_{40}] \cdot 6\ H_2O$: 44.77 % Mo, 4.33 % Nb, 1.17 % P 0.75 % K, 4.84 % Na. Data normalized to molybdenum. Na/K/P/Nb/Mo ratio: 4.96/0.45/0.893/1.10/11.

TGA: 4.933 % weight loss upon drying, this corresponds to 6 mol lattice water per mol of the POM.

Additional protocol for the nanofiltration process:

- Cycle 1: 65 mL permeate in 25 min
- Cycle 2: 70 mL permeate in 46 min
- Cycle 3: 70 mL permeate in 68 min
- Cycle 4: 70 mL permeate in 88 min

$NaPNb_2Mo$:

^{31}P-NMR (242.9 MHz, H_2O/D_2O, 20 °C): δ [ppm] = -0.28, -0.36, -1.26, -1.33, -1.40, -2.45, -2.51, -2.63, -2.92, -2.96, -3.04, -3.09, -3.19, -3.27, -3.28, -3.33, -3.37, -3.46, -2.64.

IR (ATR): $\tilde{\nu}$ [cm^{-1}] = 3412 (w, O-H, H_2O), 1613 (O-H, hydration H_2O), 1049 (w, P-O), 947 (me, M=O_t), 856 (me, (M-O-M)$_{vertex}$), 757 (st, (M-O-M)$_{edge}$).

UV-Vis [nm]: 209, 292.

ICP-OES: Calculated for $Na_5[PNb_2Mo_{10}O_{40}] \cdot 5\ H_2O$: 47.467 % Mo, 9.193 % Nb, 1.532 % P, 0.00 % K, 5.687 % Na. Found for $Na_5[PNb_2Mo_{10}O_{40}] \cdot 5\ H_2O$: 47.74 % Mo, 8.456 % Nb, 1.50 % P 1.36 % K, 4.565 % Na. Data normalized to molybdenum. Na/K/P/Nb/Mo ratio: 3.99/0.70/0.98/1.83/10.

TGA: 4.652 % weight loss upon drying, this corresponds to 5 mol lattice water per mol of the POM.

Additional protocol for the nanofiltration process:

- Cycle 1: 65 mL permeate in 22 min
- Cycle 2: 70 mL permeate in 43 min
- Cycle 3: 70 mL permeate in 63 min
- Cycle 4: 70 mL permeate in 83 min

$NaKPNb_3Mo$:

^{31}P-NMR (242.9 MHz, H_2O/D_2O, 20 °C): δ [ppm] = -2.36, -2.48, -2.52, -2.61, -2.73, -2.78, -2.91, -2.96, -3.04, -3.09, -3.18, -3.26, -3.28, -3.33, -3.37, -3.63.

IR (ATR): $\tilde{\nu}$ [cm^{-1}] = 3388 (w, O-H, H_2O), 1613 (O-H, hydration H_2O), 1047 (w, P-O), 944 (me, M=O_t), 857 (me, (M-O-M)$_{vertex}$), 760 (st, (M-O-M)$_{edge}$).

UV-Vis [nm]: 210, 292.

ICP-OES: Calculated for $Na_6[PNb_3Mo_9O_{40}] \cdot 7\ H_2O$: 41.569 % Mo, 13.418 % Nb, 1.491 % P, 0.00 % K, 6.641 % Na. Found for $Na_6[PNb_3Mo_9O_{40}] \cdot 7\ H_2O$: 38.54 % Mo, 12.03 % Nb, 1.26 % P 2.37 % K, 4.30 % Na. Data normalized to molybdenum. Na/K/P/Nb/Mo ratio: 4.19/1.36/0.91/2.90/9.

TGA: 6.297 % weight loss upon drying, this corresponds to 7 mol lattice water per mol of the POM.

Additional protocol for the nanofiltration process:

- Cycle 1: 65 mL permeate in 18 min
- Cycle 2: 70 mL permeate in 36 min
- Cycle 3: 70 mL permeate in 54 min
- Cycle 4: 70 mL permeate in 75 min

NaKPV_2NbMo:

^{31}P-NMR (242.9 MHz, H_2O/D_2O, 20 °C): δ [ppm] = -2.50 to -4.30.

^{51}V-NMR (157.8 MHz, H_2O/D_2O, 20 °C): δ [ppm] = -517.7, -525.9, -531.3, -532.8, -533.2, -533.8, -534.3, -535.7, -538.5, -540 to -546.

IR (ATR): $\tilde{\nu}$ [cm^{-1}] = 3374 (w, O-H, H_2O), 1610 (O-H, hydration H_2O), 1046 (w, P-O), 941 (me, M=O_t), 847 (me, (M-O-M)$_{vertex}$), 750 (st, (M-O-M)$_{edge}$).

UV-Vis [nm]: 208, 300.

ICP-OES: Calculated for $Na_6[PV_2NbMo_9O_{40}] \cdot 7\ H_2O$: 43.319 % Mo, 4.661 % Nb, 5.111 % V, 1.554 % P, 0.00 % K, 6.92 % Na. Found for $Na_6[PV_2NbMo_9O_{40}] \cdot 7\ H_2O$: 38.50 % Mo,

4.38 % Nb, 5.225 % V 1.52 % P 1.38 % K, 6.49 % Na. Data normalized to molybdenum. Na/K/P/V/Nb/Mo ratio: 6.33/0.792/1.10/2.3/1.06/9.

TGA: 5.901 % weight loss upon drying, this corresponds to 7 mol lattice water per mol of the POM.

Additional protocoll for the nanofiltration process:

- Cycle 1: 65 mL permeate in 29 min
- Cycle 2: 70 mL permeate in 63 min
- Cycle 3: 70 mL permeate in 92 min
- Cycle 4: 70 mL permeate in 122 min

$NaKPVNb_2Mo$:

^{31}P-NMR (242.9 MHz, H_2O/D_2O, 20 °C): δ [ppm] = -4.92, -5.08, -5.27 to -5.36, -5.49, -5.62, -5.69, -5.93, -5.96, -5.99, -6.04, -6.20, -6.30, -6.42, -6.43, -6.49, -6.54, -6.73, -6.77, -6.86, -6.88, -6.89, -6.90.

^{51}V-NMR (157.8 MHz, H_2O/D_2O, 20 °C): δ [ppm] = -519.8, -527.9, -532.7, -533.7, -534.4, -535.4, -537.1, -545.1.

IR (ATR): $\tilde{\nu}$ [cm^{-1}] = 3391 (w, O-H, H_2O), 1615 (O-H, hydration H_2O), 1048 (w, P-O), 944 (me, M=O_t), 859 (me, (M-O-M)$_{vertex}$), 762 (st, (M-O-M)$_{edge}$).

UV-Vis [nm]: 209, 297.

ICP-OES: Calculated for $Na_6[PVNb_2Mo_9O_{40}] \cdot 5\ H_2O$: 43.191 % Mo, 9.294 % Nb, 2.548 % V, 1.549 % P, 0.00 % K, 6.90 % Na. Found for $Na_6[PVNb_2Mo_9O_{40}] \cdot 5\ H_2O$: 42.28 % Mo, 8.915 % Nb, 2.19 % V 1.46 % P 1.545 % K, 4.645 % Na. Data normalized to molybdenum. Na/K/P/V/Nb/Mo ratio: 4.13/0.81/0.964/0.880/1.96/9.

TGA: 4.077 % weight loss upon drying, this corresponds to 5 mol lattice water per mol of the POM.

Additional protocol for the nanofiltration process:

- Cycle 1: 65 mL permeate in 20 min
- Cycle 2: 70 mL permeate in 41 min

- Cycle 3: 70 mL permeate in 63 min
- Cycle 4: 70 mL permeate in 81 min

$NaPV_3Mo$:

^{31}P-NMR (242.9 MHz, H_2O/D_2O, 20 °C): δ [ppm] = -0.15, -2.70, -2.96, -3.02, -3.06, 3.26, -3.34, -3.42, -3.49, -3.52, -3.56, -3.62, -3.72, -4.05, -4.06, -4.13, -4.20, -4.21.

^{51}V-NMR (157.8 MHz, H_2O/D_2O, 20 °C): δ [ppm] = -521.1, -532.0, -533.3, -533.6, -535.2, -536.8, -535.9, -540.8, -541.3, -542.9, -544, -547.8, -549.4.

IR (ATR): $\tilde{\nu}$ [cm^{-1}] = 3561, 3307 (w, O-H, H_2O), 1618 (O-H, hydration H_2O), 1064, 1048 (w, P-O), 937 (me, M=O_t), 846 (me, (M-O-M)$_{vertex}$), 758 (st, (M-O-M)$_{edge}$).

UV-Vis [nm]: 214, 308.

ICP-OES: Calculated for $Na_6[PV_3Mo_9O_{40}] \cdot 8\ H_2O$: 43.846 % Mo, 7.76 % V, 1.573 % P, 0.00 % K, 7.004 % Na. Found for $Na_6[PV_3Mo_9O_{40}] \cdot 8\ H_2O$: 46.88 % Mo, 8.205 % V 1.61 % P 0.00 % K, 6.75 % Na. Data normalized to molybdenum. Na/K/P/V/Mo 5.41/0/0.957/2.97/9

TGA: 7.128 % weight loss upon drying, this corresponds to 8 mol lattice water per mol of the POM.

$NaPW_3Mo$:

^{31}P-NMR (242.9 MHz, H_2O/D_2O, 20 °C): δ [ppm] = 0.61 (**P**O_4^{3-}), -1.63 to -12.45.

IR (ATR): $\tilde{\nu}$ [cm^{-1}] = 3464, 3307 (w, O-H, H_2O), 1620 (O-H, hydration H_2O), 1058 (w, P-O), 964 (me, M=O_t), 909, 865 (me, (M-O-M)$_{vertex}$), 799 (st, (M-O-M)$_{edge}$).

UV-Vis [nm]: < 200.

ICP-OES: Calculated for $Na_3[PW_3Mo_9O_{40}] \cdot 28\ H_2O$: 32.469 % Mo, 20.739 % W, 1.165 % P, 0.00 % K, 2.593 % Na. Found for $Na_3[PW_3Mo_9O_{40}] \cdot 28\ H_2O$: 32.0 % Mo, 20.62 % W 1.20 % P 0.01 % K, 4.61 % Na. Data normalised to molybdenum. Na/K/P/W/Mo ratio: 4.88/0.00690/1.05/3.03/9.

TGA: 19.15 % weight loss upon drying, this corresponds to 28 mol lattice water per mol of the POM.

Additional protocol for the nanofiltration process:

- Cycle 1: 65 mL permeate in 25 min
- Cycle 2: 70 mL permeate in 47 min
- Cycle 3: 70 mL permeate in 68 min
- Cycle 4: 70 mL permeate in 90 min

1.8 Computational Methods

All DFT calculations were performed using TURBOMOLE v. 7.5.1 2021.[14] Structures were optimized using the PBE0 hybrid functional[15] using an Ahlrichs'triple-ξ valence polarization (def2-TZVP) basis set for all atoms.[16] The resolution of identity approximation was applied using the corresponding auxiliary def2-TZVP basis set to approximate the Coulomb potentials. Geometry optimizations were carried out in gas phase with strict scf convergence criteria (10^{-8}) and a fine m4 grid. Each optimized structure was characterized to be a minimum by absence of any imaginary frequency. IR and Raman spectra are displayed 'as calculated' without any scaling factor. Thermodynamic corrections for all species were evaluated at 298 K and 1 bar within the rigid-rotor harmonic-oscillator approximation. The implicit COSMO[17] (Conductor like Solvation MOdel) for water was used to consider solvation effects.

Cartesian coordinates of the optimized structures in Å

LHPA-3

Mo	4.9128525	1.3010269	2.2832149
Mo	8.2145369	0.6924210	2.0301763
Mo	7.6612561	5.9560831	5.0679291
P	7.0444109	4.0460266	2.1996211
O	6.7671426	2.6024777	1.7513330
O	7.0372216	4.0541309	3.7633554
O	7.8942395	7.1241158	6.2478147
O	5.9601333	5.1216517	5.8488260
O	6.2991625	0.1601465	2.4653000
O	9.5672377	1.8332170	1.7726079
O	3.5862828	0.2699677	2.3720676
O	7.6460321	0.4935344	0.2525159
O	8.1142001	1.3311517	3.8754795

O	5.0722152	1.2303405	0.2711932
O	8.9884334	-0.7751590	2.2698572
O	4.9698971	2.0967253	3.9120548
O	8.4198767	4.5185533	1.7381396
O	5.9354884	4.9836174	1.7138934
Mo	10.5837680	3.5396628	2.2914661
Mo	9.3983699	6.7012827	1.9417749
Mo	5.1583447	3.6511849	5.1783555
O	4.0103171	3.2608089	6.3357536
O	6.6692254	2.5711666	5.8386373
O	10.8361426	5.3172228	2.3894427
O	7.7415543	7.3230953	1.7467773
O	12.1308752	2.9298087	2.5159044
O	9.8446058	6.2665978	0.1829759
O	8.9407866	6.3290270	3.8343238
O	10.5627292	3.6786321	0.3017256
O	10.2970372	8.0996917	2.1540683
O	9.8033025	3.2476758	3.9124682
Mo	5.7550416	7.3987487	2.2197673
Mo	3.6262835	4.7634116	2.0516991
Mo	8.3776465	2.6292086	5.1483618

Mo	2.6540861	-0.9939516	7.0270233
Mo	4.7341535	-1.9126923	4.4850736
P	5.5286806	5.4646117	4.7635737
P	4.0404707	1.5332942	4.9621201
O	4.0241483	5.5497683	5.0408101
O	6.2612192	4.7446824	5.9003553
O	5.8059175	4.7937519	3.4144154
O	6.0837082	6.9303076	4.6903322
O	1.9529450	6.8993674	5.4533395
O	4.4066327	5.5428321	7.8518583
O	7.9562999	4.7397314	7.7471995
O	8.3430856	3.8697222	4.1847434
O	6.7225390	4.8750598	1.0838001
O	3.3411169	5.6719774	2.3206936
O	3.6433989	7.9799696	3.5296217
O	4.1917554	7.8455097	6.6638146
O	6.4966906	7.0981227	7.5538033
O	8.7111967	6.0762331	5.5090971
O	8.2920907	6.1903417	2.9636977
O	5.4454603	7.1328882	1.8863594
O	5.4016643	9.4412097	4.7840066
O	7.7145888	8.6172585	5.8182492
O	7.3623037	8.6181010	3.1765900
O	1.5098756	4.7419652	3.9246661
O	2.0414716	4.5939644	6.9632968
O	5.7389406	3.3612855	8.3568784
O	7.8762579	2.3524416	6.3687108
O	7.1533704	2.5229933	2.2989031
O	4.3880009	3.4188087	1.2609511

O	2.8676532	2.4893602	5.2028695
O	5.1083212	1.6824012	6.0507841
O	4.6404380	1.7328626	3.5666009
O	3.4849340	0.0679721	5.0367880
O	0.4359795	2.8877528	5.6607511
O	3.2059921	2.5023337	7.9928330
O	6.4408073	0.7268451	7.9463657
O	7.1925506	0.8081154	4.3850610
O	5.1995205	0.8630646	1.2842697
O	2.2171113	2.5979303	2.4434822
O	0.9548890	0.8718812	3.9226016
O	1.5122573	0.7356009	7.0525466
O	3.8339835	-0.0187207	7.8963106
O	6.0370734	-1.0428566	5.8395245
O	5.5711661	-0.9133460	3.3032793
O	2.7236758	0.0323775	2.2391085
O	1.3486329	-1.3471915	5.4926656
O	3.7484565	-2.2187109	6.2535382
O	3.1269686	-2.1154132	3.6633708
O	1.1214668	7.2932501	2.8672278
O	2.0510340	6.9783831	8.1900987
O	6.3983941	5.6409784	9.8199222
O	10.1147334	3.8309346	6.3241204
O	9.3178309	4.1217438	1.5708364
O	4.4437609	5.6484783	-0.2290551
O	5.8023644	9.9038097	7.4725182
O	9.9460259	8.1756444	4.2618530
O	5.2082552	9.8568892	1.9828845
O	-0.4396402	3.1062131	3.0738820
O	0.4516298	2.8129929	8.4045562
O	4.8076954	1.4717990	10.0173482
O	8.5430437	-0.3499328	6.5490717
O	7.7324959	-0.0480477	1.7981023
O	2.8708760	1.4698392	-0.0366160
O	0.4385313	-1.6139488	2.9055335
O	1.8573268	-1.8797521	8.2315817
O	5.4467354	-3.4429811	4.3382750

$[PMo_{12}O_{40}]^{-3}$

O	-0.8301282	4.2498370	20.9158558
O	0.7790832	3.3097849	23.1694028
Mo	0.9893851	-0.0971768	19.7037802
O	5.9726430	1.9058505	22.3734621
O	-4.4152602	2.1460484	22.7164288
O	-0.5656007	5.0552603	24.5322718
O	-2.6554930	-0.0442710	22.4390694
O	0.8428032	5.7955742	22.4399589
O	2.0872030	-0.7473277	20.9910982
Mo	-0.9613395	0.6183535	25.4964723

O	0.7325321	-1.4737585	23.0499818
O	-2.0621961	3.2662412	18.5331207
Mo	-1.0278911	2.6671498	19.7037253
O	3.1310979	-2.7720573	22.7167164
O	-0.4709450	1.1438619	23.1692797
O	-2.1388561	2.0405477	20.9920870
O	-1.8492934	6.3452180	22.3743713
O	2.0608168	5.0194443	24.6359011
O	0.5699747	4.7065678	27.0119595
Mo	2.7308976	0.9824469	25.4973009
O	-0.4806507	-0.7200386	20.9142240
O	3.6975507	3.4972554	23.0505756
O	-1.7810631	-2.6512493	22.3744348
Mo	2.5853110	4.9195274	22.8889406
O	4.1510233	-0.1531361	22.4399234
O	3.3439870	0.6281393	27.0131595
Mo	0.5703074	3.9978189	25.4965413
Mo	-1.1711637	-1.1029418	22.5460836
O	-1.5748963	0.2664512	27.0126831
O	2.0299268	1.1449323	23.1694320
O	-0.5030953	1.0539129	19.0268380
Mo	4.3264688	1.6621814	22.5459691
O	-2.0935619	3.5784598	23.0500074
Mo	-0.8168610	5.0403995	22.5472835
O	2.3884545	4.3048486	20.9918305
O	3.6489951	2.0681840	20.9148487
O	-1.3101387	-0.8936931	24.5331252
Mo	2.5206927	-1.2240884	22.8896329
O	4.2138194	1.4368633	24.5328056
O	2.1246389	1.1640751	19.0264595
O	3.6172689	6.2247003	22.7156834
Mo	2.3748441	3.0309234	19.7022241
O	3.4097660	3.6292911	18.5317752
O	2.0409430	2.6486794	25.6811580
O	0.8270058	0.3836576	25.6801092
O	2.8691190	-0.8205090	24.6364692
P	0.7792496	1.8660841	22.6586287
O	-0.5265881	2.5667145	25.6791002
O	0.7785628	1.8659200	21.1270724
O	0.9885488	-1.2901990	18.5312837
O	-2.5916263	1.3991011	24.6357598
O	0.7153212	3.3834151	19.0259439
Mo	-2.7688575	1.9041557	22.8892264

$[PMo_{11}CoO_{40}]^{-7}$

O	0.0052418	1.2863145	-3.6800646
O	1.9699480	3.2199196	-0.6143543
O	-0.0926238	5.1493326	-0.0494637
O	0.9636086	-3.6063564	1.9393325

O 2.0619690 -0.0472550 2.6601165
O 3.2922733 -0.0795938 -0.3602121
Mo -1.5410381 1.6254840 -2.7743475
O -0.1263215 -1.4125457 3.1289249
Mo 1.4531961 -0.1017454 -3.2135793
O 2.2477216 1.1931210 -2.2790192
O -2.4820938 -2.7412471 -3.8329207
O -1.3207958 -0.1654457 0.8019751
Mo 1.5548012 1.6804038 2.6684781
O -2.7682692 1.2988227 2.4359681
Mo -1.6070258 -0.0882797 3.1928864
O 0.8295928 -1.4068477 0.4117978
O 2.2303811 -1.4198358 -2.2667857
O -0.2490312 -0.1506832 -1.4766970
O -0.1381482 1.2505313 3.2015663
O -2.7019249 -1.6187728 -1.1955615
O 2.2556896 -2.5415527 4.0719706
O 2.2702188 2.3442735 4.0810023
Mo 3.0737699 1.7742138 -0.4133429
O -0.6665192 -3.1495423 -1.8362370
O 3.1744786 1.9668598 1.3826101
Co 0.1312437 -3.8501766 -0.0239718
O -4.4825043 -2.8446887 0.6579856
O 2.2860408 -0.1074351 -4.7146537
Mo 0.0315707 3.4399123 0.0695634
O 4.6123197 -2.5134471 -0.9279724
O 4.5929849 2.3586859 -0.9609614
Mo -3.1932576 1.5788307 0.6297871
O -2.3449652 2.7560867 -3.7849251
O -0.0461777 -5.7602078 -0.1306177
O 3.1227120 -2.1282886 1.3998795
O -1.5236557 2.9233998 0.7721537
O -2.2823952 0.0588725 -3.2059422
Mo -1.5079052 -1.8968174 -2.6952713
O 2.1010822 -3.5108221 -0.6626251
Mo 3.0348659 -2.0432380 -0.4404190
O -0.0767631 -1.3177089 -3.7313976
O -2.0877458 -0.1186787 4.8227033
O -2.6486502 1.6792065 -1.1465222
O -4.0176742 0.0271463 0.4656812
O -4.4706132 2.7232873 0.7285442
O 0.9455471 3.2696716 1.7785490
O -2.8476541 -1.4113425 2.4153254
Mo 1.5022311 -2.0808712 2.5993880
O 0.7951277 1.1252356 0.4170324
O -0.4492200 2.8433581 -1.5954463
O -1.7833815 -3.2250821 0.6911808
P 0.0237558 -0.1552110 0.0399461
Mo -2.9933424 -1.9845943 0.6357047

$[PMo_{11}FeO_{40}]^{-6}$

O	0.1018818	1.2690916	-3.7680417
O	1.9145590	3.2041140	-0.6340538
O	-0.1114766	5.0992492	-0.1510562
O	0.8222310	-3.4342720	1.8726973
O	1.9369294	-0.1769270	2.7239347
O	3.3448291	-0.1406303	-0.2689018
Mo	-1.6602250	1.6446340	-2.6581117
O	-0.2346278	-1.4519292	3.2682450
Mo	1.3776452	0.0820565	-3.3449334
O	2.2915587	1.1574110	-2.1962770
O	-2.2653227	-2.8208782	-3.7944734
O	-1.3167503	-0.1070203	0.7976839
Mo	1.5249115	1.7040054	2.6573702
O	-2.8055117	1.3313780	2.5297112
Mo	-1.5015777	-0.2231298	3.2810234
O	0.7866958	-1.4002064	0.3356665
O	2.2689250	-1.4055971	-2.2398745
O	-0.2863337	-0.0695966	-1.4975966
O	-0.2830660	1.1773898	3.1495532
O	-2.7113353	-1.5714533	-1.2575350
O	2.3905946	-2.6441964	3.9968816
O	2.1692791	2.3599420	4.0779666
Mo	3.0594189	1.6774142	-0.3996243
O	-0.5558217	-2.9634466	-1.6509262
O	3.0826953	1.9611123	1.4022315
Fe	0.1131184	-3.4356788	0.1007559
O	-4.4025103	-2.7528321	0.6556713
O	2.3536929	0.0328080	-4.7416394
Mo	0.1133296	3.4229021	0.0272897
O	4.4695658	-2.6620297	-1.1184116
O	4.5672097	2.2970610	-0.8892074
Mo	-3.1166903	1.6669083	0.8096551
O	-2.3789767	2.7078129	-3.7825947
O	-0.1755041	-5.0142403	0.0021706
O	3.1365005	-2.1770920	1.3593899
O	-1.5739606	2.8124298	0.6258855
O	-2.1155031	-0.0276742	-3.2976362
Mo	-1.4082193	-1.8309397	-2.7012914
O	1.9132772	-3.5082390	-0.5618735
Mo	2.9386302	-2.0468214	-0.6867387
O	0.1092066	-1.3575868	-3.7153444
O	-2.0296466	-0.1641012	4.9037628
O	-2.7796331	1.6522957	-1.2773332
O	-3.8996606	0.0575419	0.4771990
O	-4.4189565	2.7696996	0.8416315
O	0.7796698	3.3079884	1.7489482
O	-2.8372070	-1.2813430	2.4630884
Mo	1.7520096	-2.0387822	2.5344719
O	0.8320506	1.1065712	0.4114325

O	-0.4610984	2.7490482	-1.6773624
O	-1.6567443	-2.9383680	0.7114608
P	-0.0005880	-0.1168965	0.0093291
Mo	-2.9906227	-1.7966742	0.5773113

$[PMo_{11}InO_{40}]^{-6}$

O	0.1587737	1.3271914	-3.7249133
O	1.8256643	3.3452149	-0.5349308
O	-0.2119001	5.1431227	0.0654313
O	0.8614428	-3.6012943	1.9000104
O	2.0619839	-0.0443686	2.7173756
O	3.3475238	0.0324889	-0.2410113
Mo	-1.3907765	1.7302372	-2.8012600
O	-0.1682972	-1.3538029	3.0880570
Mo	1.3834386	-0.1757672	-3.3049663
O	2.2520574	1.2989259	-2.2275694
O	-2.5143986	-2.6240635	-3.7905224
O	-1.2946360	-0.0927399	0.7809789
Mo	1.7676026	1.7002410	2.5987405
O	-2.7485334	1.2775913	2.5032257
Mo	-1.5508071	0.1129050	3.1887715
O	0.8685840	-1.3294016	0.4121380
O	2.2767537	-1.2754096	-2.1687094
O	-0.2385920	-0.1038894	-1.4865346
O	-0.1266810	1.2278659	3.1513779
O	-2.7756507	-1.5912826	-1.2097646
O	2.1489228	-2.5579353	4.0406015
O	2.3681894	2.3495762	4.0554881
Mo	2.9749639	1.7470816	-0.6266458
O	-0.6268976	-3.0046864	-1.8545265
O	3.0666585	2.1120599	1.3973274
In	0.0196970	-4.2337993	-0.1010386
O	-4.4487308	-2.7562768	0.8337972
O	2.3556080	-0.1510519	-4.6993263
Mo	0.0917069	3.4735516	0.1878055
O	4.5587232	-2.4447133	-0.8890132
O	4.4722047	2.4494591	-1.0369131
Mo	-3.1135852	1.6383959	0.4893679
O	-2.1723970	2.8222337	-3.8466649
O	-0.1701107	-6.1513512	-0.2531572
O	3.0597777	-2.1255663	1.4088603
O	-1.5772770	2.7862305	0.7326354
O	-2.1136415	0.0990057	-3.2430732
Mo	-1.6249395	-1.7804953	-2.6093609
O	2.0694014	-3.4963474	-0.7032988
Mo	2.9756476	-2.0263647	-0.4237015
O	0.0436057	-1.2966158	-3.7610021
O	-1.9682900	0.0533790	4.8360519
O	-2.7639756	1.6648305	-1.2729797

O	-3.8860281	-0.0019109	0.5498912
O	-4.4289145	2.7052657	0.6673265
O	0.7798015	3.3116227	1.8848617
O	-2.7389249	-1.3556895	2.5206987
Mo	1.4216452	-2.0860150	2.5741231
O	0.8346090	1.1763320	0.3874375
O	-0.5169327	2.8212415	-1.5835120
O	-1.7500250	-3.0843680	0.6699645
P	0.0484381	-0.1012764	0.0266486
Mo	-2.9996602	-1.8672845	0.7669889

$[PMo_{11}NiO_{40}]^{-5}$

O	0.1587737	1.3271914	-3.7249133
O	1.8256643	3.3452149	-0.5349308
O	-0.2119001	5.1431227	0.0654313
O	0.8614428	-3.6012943	1.9000104
O	2.0619839	-0.0443686	2.7173756
O	3.3475238	0.0324889	-0.2410113
Mo	-1.3907765	1.7302372	-2.8012600
O	-0.1682972	-1.3538029	3.0880570
Mo	1.3834386	-0.1757672	-3.3049663
O	2.2520574	1.2989259	-2.2275694
O	-2.5143986	-2.6240635	-3.7905224
O	-1.2946360	-0.0927399	0.7809789
Mo	1.7676026	1.7002410	2.5987405
O	-2.7485334	1.2775913	2.5032257
Mo	-1.5508071	0.1129050	3.1887715
O	0.8685840	-1.3294016	0.4121380
O	2.2767537	-1.2754096	-2.1687094
O	-0.2385920	-0.1038894	-1.4865346
O	-0.1266810	1.2278659	3.1513779
O	-2.7756507	-1.5912826	-1.2097646
O	2.1489228	-2.5579353	4.0406015
O	2.3681894	2.3495762	4.0554881
Mo	2.9749639	1.7470816	-0.6266458
O	-0.6268976	-3.0046864	-1.8545265
O	3.0666585	2.1120599	1.3973274
In	0.0196970	-4.2337993	-0.1010386
O	-4.4487308	-2.7562768	0.8337972
O	2.3556080	-0.1510519	-4.6993263
Mo	0.0917069	3.4735516	0.1878055
O	4.5587232	-2.4447133	-0.8890132
O	4.4722047	2.4494591	-1.0369131
Mo	-3.1135852	1.6383959	0.4893679
O	-2.1723970	2.8222337	-3.8466649
O	-0.1701107	-6.1513512	-0.2531572
O	3.0597777	-2.1255663	1.4088603
O	-1.5772770	2.7862305	0.7326354
O	-2.1136415	0.0990057	-3.2430732

Mo	-1.6249395	-1.7804953	-2.6093609
O	2.0694014	-3.4963474	-0.7032988
Mo	2.9756476	-2.0263647	-0.4237015
O	0.0436057	-1.2966158	-3.7610021
O	-1.9682900	0.0533790	4.8360519
O	-2.7639756	1.6648305	-1.2729797
O	-3.8860281	-0.0019109	0.5498912
O	-4.4289145	2.7052657	0.6673265
O	0.7798015	3.3116227	1.8848617
O	-2.7389249	-1.3556895	2.5206987
Mo	1.4216452	-2.0860150	2.5741231
O	0.8346090	1.1763320	0.3874375
O	-0.5169327	2.8212415	-1.5835120
O	-1.7500250	-3.0843680	0.6699645
P	0.0484381	-0.1012764	0.0266486
Mo	-2.9996602	-1.8672845	0.7669889

$[PMo_{11}VO_{40}]^{-4}$

O	0.1485867	1.2537809	-3.7194954
O	1.8814303	3.3232053	-0.5527801
O	-0.2098787	5.1034221	0.1056142
O	0.7441777	-3.5273878	1.7127265
O	2.0250131	-0.1579835	2.7016786
O	3.3204569	-0.0728897	-0.2482496
Mo	-1.3362925	1.7025930	-2.7557004
O	-0.2100881	-1.3657847	3.1112615
Mo	1.3917719	-0.2675552	-3.3082136
O	2.2505837	1.1921229	-2.2120812
O	-2.4692737	-2.7122628	-3.7150730
O	-1.3280416	-0.0665251	0.7671857
Mo	1.7701738	1.6228788	2.5661492
O	-2.7659801	1.2740887	2.4719440
Mo	-1.5634137	0.1086067	3.1943123
O	0.8105999	-1.3132093	0.3909389
O	2.2585282	-1.3781749	-2.1823269
O	-0.2625842	-0.0715083	-1.4986058
O	-0.1162567	1.2032413	3.1083599
O	-2.7660499	-1.6413364	-1.1899164
O	2.0125044	-2.7222182	4.0063044
O	2.3983668	2.2391512	4.0004929
Mo	2.9230887	1.8253236	-0.6579338
O	-0.5516239	-2.8879866	-1.6839336
O	3.0844817	1.9668357	1.3495653
V	0.1756770	-3.5932610	-0.1546980
O	-4.2831015	-2.9145375	0.8668039
O	2.3486192	-0.2465600	-4.6931465
Mo	0.0266000	3.4426406	0.2394898
O	4.5197938	-2.4919117	-0.8501079
O	4.4348827	2.4266435	-1.0870654

Mo	-3.1424656	1.5378592	0.5084529
O	-2.1455272	2.7663037	-3.7774954
O	-0.0963049	-5.1309955	-0.3051965
O	3.0029392	-2.2109041	1.4239418
O	-1.5919792	2.8100429	0.7441944
O	-2.1283789	0.0149104	-3.2386691
Mo	-1.6526563	-1.7217198	-2.6266097
O	1.8811788	-3.4231146	-0.6310194
Mo	3.0244012	-1.8838869	-0.3756824
O	0.0238404	-1.3689953	-3.7474751
O	-1.9667129	0.0983908	4.8274342
O	-2.6820949	1.5717014	-1.2326279
O	-3.9171129	-0.1000990	0.5533112
O	-4.4488254	2.5944805	0.6122969
O	0.8555805	3.2705946	1.8664795
O	-2.7249968	-1.3573091	2.5318814
Mo	1.3741389	-2.0848367	2.5843675
O	0.8088674	1.1801571	0.3822432
O	-0.4675952	2.8114472	-1.5713727
O	-1.5534412	-2.9711425	0.6413596
P	0.0069439	-0.0747463	0.0098334
Mo	-2.9497061	-1.8892964	0.7784329

$[PMo_{11}NbO_{40}]^{-4}$

O	-1.9256808	0.5715342	-3.3850107
O	-0.4637654	3.7535783	-1.1254789
O	-2.8614035	4.3304410	0.1095220
O	3.0617950	-2.1261851	1.3147609
O	2.4289677	1.4434542	1.7203819
O	2.5615600	1.6326147	-1.5033301
Mo	-3.0887798	0.1413657	-1.7819091
O	1.6392049	-0.6488396	2.9293664
Mo	-0.1998645	0.0510302	-3.6014272
O	0.3359536	1.8443415	-2.8346271
O	-1.7408670	-4.1741573	-2.6317345
O	-0.7201698	-0.4891971	1.2586132
Mo	1.1717472	2.8771264	1.7685834
O	-1.9710972	0.1814730	3.4531851
Mo	0.0368406	-0.1347157	3.5592755
O	1.4143752	-0.6137628	-0.0456846
O	1.6540313	-0.3119996	-2.9269102
O	-0.7729625	-0.4419951	-1.2500996
O	0.2631312	1.5718633	3.0321422
O	-1.7557335	-2.9462584	-0.1646883
O	4.4723257	-0.1823152	2.6898303
O	1.8317547	3.9413871	2.8906443
Mo	1.2412056	2.8750266	-1.6578924
O	0.5104825	-3.0564475	-1.4851328
O	1.7678283	3.5345210	0.1776358

Nb	1.9416508	-3.0316316	-0.0527204
O	-1.8344865	-4.3167887	2.3712631
O	0.0964159	0.3203554	-5.2352731
Mo	-1.7463384	3.0753444	0.0144153
O	4.4059520	-0.0764406	-2.8049868
O	1.9199226	4.0928407	-2.6012329
Mo	-2.9867808	0.1432129	1.9497142
O	-4.5993887	0.4953512	-2.4330599
O	2.5951421	-4.6219151	-0.0972967
O	3.9471168	0.0058319	-0.0068908
O	-2.4719169	1.7990974	1.3338786
O	-2.8327190	-1.6141118	-2.2568135
Mo	-1.2386054	-2.7607932	-1.8665497
O	3.1079782	-2.0535446	-1.4192825
Mo	3.0773185	-0.2755831	-1.7942914
O	-0.5543360	-1.7124625	-3.5134154
O	0.2343210	-0.0901594	5.2309922
O	-3.4009738	-0.1423348	-0.0398555
O	-2.8673104	-1.7736986	1.9231530
O	-4.5474903	0.3875101	2.5280063
O	-0.5356588	3.5546213	1.4890985
O	-0.6475430	-2.0386437	3.3611732
Mo	3.1786159	-0.2988459	1.6226779
O	0.1122900	1.5230542	0.0217321
O	-2.4627197	1.9390519	-1.2283733
O	0.4010479	-3.1729189	1.1643328
P	0.0085962	-0.0075548	-0.0018730
Mo	-1.2863861	-2.8151277	1.8493656

$[PMo_{11}WO_{40}]^{-3}$

O	0.1331552	1.2380096	-3.7166771
O	1.8629096	3.3283368	-0.5396216
O	-0.2185810	5.1038006	0.1379699
O	0.7659580	-3.5307791	1.7406721
O	2.0302717	-0.1621313	2.6971252
O	3.3416297	-0.0607145	-0.2450426
Mo	-1.3249773	1.7414438	-2.7504987
O	-0.1996374	-1.3727535	3.1070266
Mo	1.3824669	-0.2777365	-3.2897177
O	2.2307817	1.1865364	-2.2030659
O	-2.5161598	-2.6679128	-3.7430516
O	-1.3263801	-0.0746067	0.7700773
Mo	1.7759476	1.6410954	2.5653466
O	-2.7703232	1.2544965	2.4594825
Mo	-1.5552714	0.1121938	3.1929376
O	0.7801733	-1.3520741	0.3564129
O	2.2585843	-1.3796823	-2.1546798
O	-0.2823746	-0.0671366	-1.5052557
O	-0.1076937	1.1932085	3.1126698

O	-2.7291507	-1.6611807	-1.1917627
O	2.0390624	-2.6705474	4.0366537
O	2.4066339	2.2397934	3.9942222
Mo	2.9169502	1.8319168	-0.6607547
O	-0.5446229	-2.9198382	-1.7122145
O	3.0816578	1.9732808	1.3466956
W	0.1415632	-3.6102880	-0.1352408
O	-4.3099802	-2.8791906	0.8553150
O	2.3331140	-0.2682546	-4.6666944
Mo	0.0385977	3.4550245	0.2493757
O	4.5634655	-2.4588512	-0.8337082
O	4.4110498	2.4407241	-1.1035208
Mo	-3.1188848	1.5475101	0.4995045
O	-2.1255869	2.7965687	-3.7726003
O	-0.1289035	-5.2845960	-0.2935866
O	3.0020165	-2.1954993	1.4210285
O	-1.5847069	2.7912157	0.7378339
O	-2.1611487	0.0239052	-3.2690849
Mo	-1.6986877	-1.6617209	-2.6863794
O	1.9336373	-3.4449574	-0.6330549
Mo	3.0698328	-1.8622696	-0.3760061
O	0.0038280	-1.3831803	-3.7262496
O	-1.9627851	0.0938784	4.8154571
O	-2.6663630	1.5632346	-1.2457061
O	-3.9049658	-0.1169804	0.5299381
O	-4.4242926	2.5891990	0.5951599
O	0.8515032	3.2622753	1.8822575
O	-2.7290008	-1.3731775	2.5212696
Mo	1.4108910	-2.0394376	2.6217325
O	0.8192052	1.1492290	0.3810931
O	-0.4669938	2.8374429	-1.5739005
O	-1.5581902	-2.9918183	0.6605131
P	-0.0035150	-0.0827851	-0.0012698
Mo	-2.9928646	-1.8519361	0.7831539

2 Additional data

In Figure S10 the principle of the TBA POM precipitation is shown:

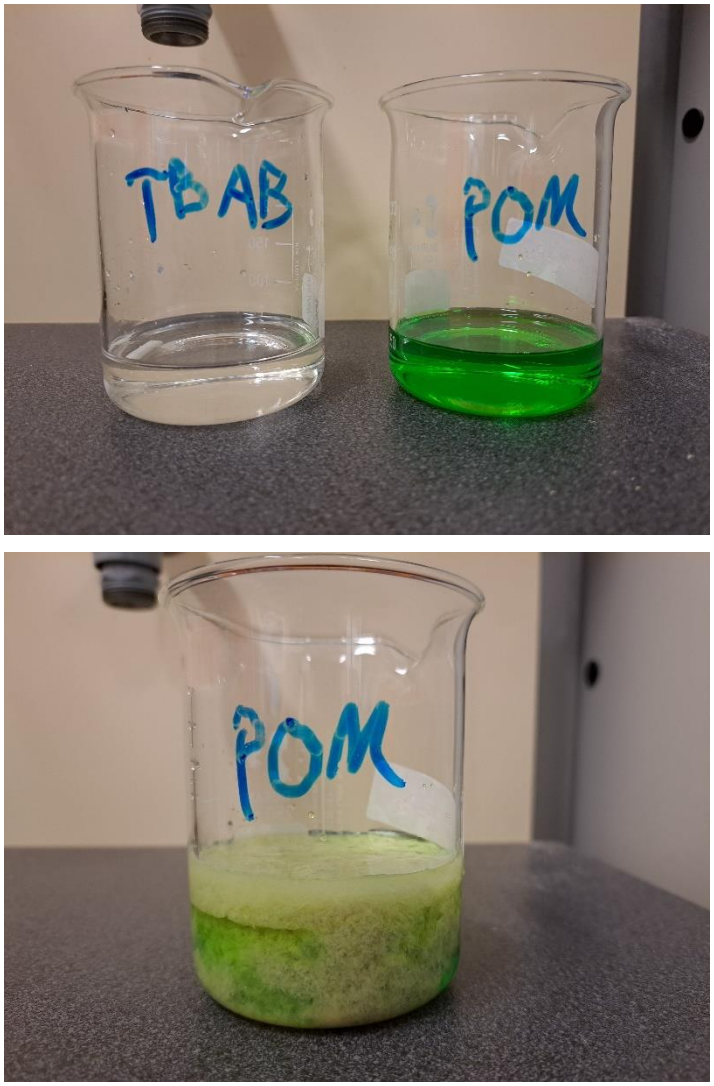

Figure S10: Aqueous TBAB solution (left) and aqueous PCu_2Mo solution (right).

2.1 Vibrational spectroscopy

2.1.1 Infrared- and Raman-spectra of transition metal substituted Keggin POMs

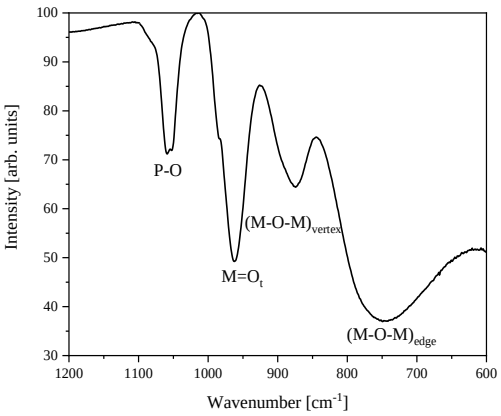

Figure S11: ATR-FT-IR spectrum of HPMo with the characteristic vibration bands.

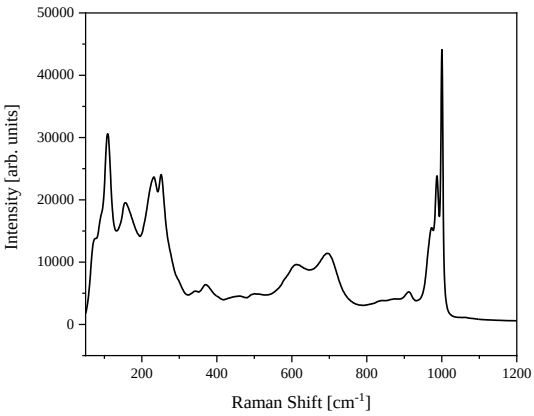

Figure S12: Raman spectrum of HPMo.

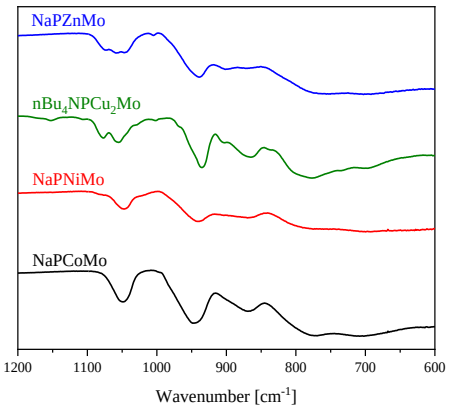

Figure S13: ATR-FT-IR spectra of the with divalent elements substituted POMs.

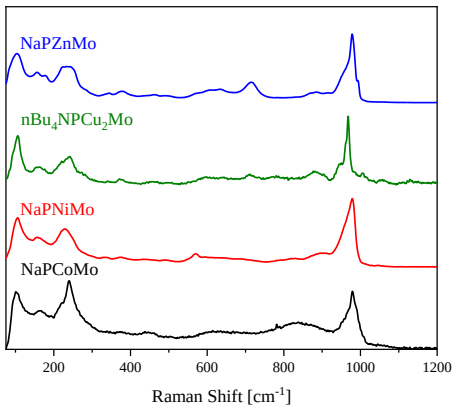

Figure S14: Raman spectra of the with divalent elements substituted POMs.

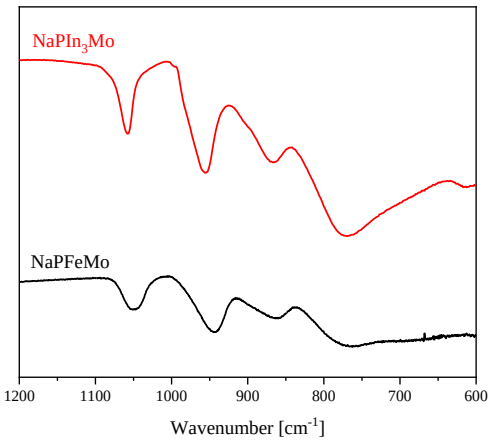

Figure S15 ATR-FT-IR spectra of the with trivalent elements substituted POMs.

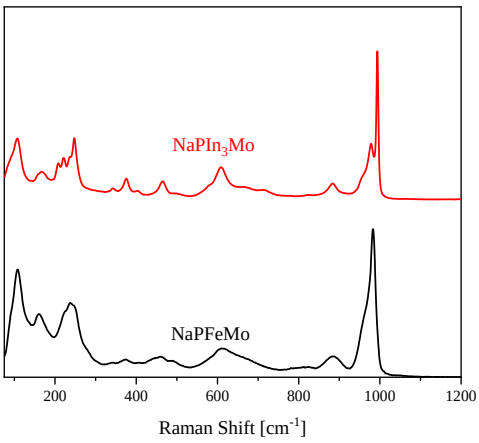

Figure S16: Raman spectra of the with trivalent elements substituted POMs.

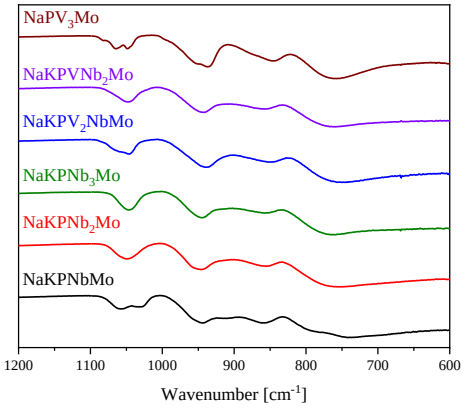

Figure S17: ATR-FT-IR spectra of the with pentavalent elements substituted POMs.

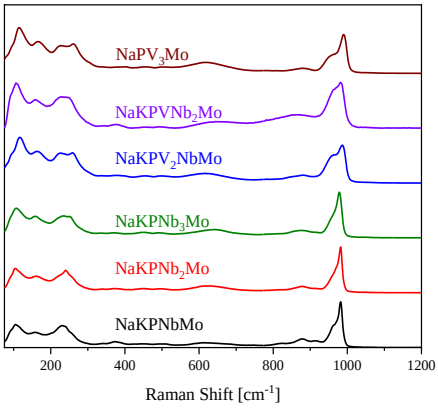

Figure S18: Raman spectra of the with pentavalent elements substituted POMs.

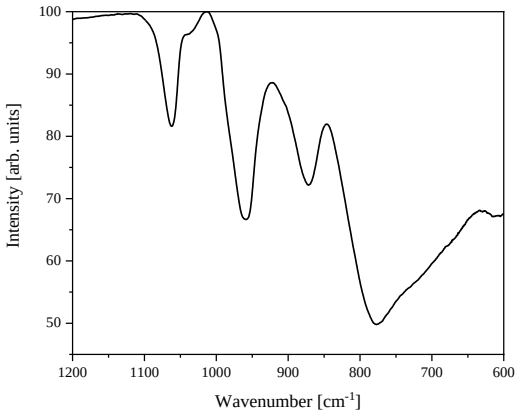

Figure S19: ATR-FT-IR spectra of the with hexavalent elements substituted POM.

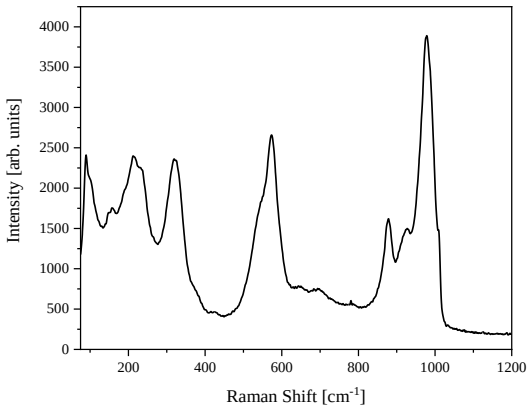

Figure S20: Raman spectra of the with hexavalent elements substituted POMs.

2.1.2 Assignment of peaks to structural features/vibration modes

Table 5: Assignment of the FT-IR peaks of each POM to the corresponding vibration modes.

POM	P-O	$M=O_t$	$(M\text{-}O\text{-}M)_{vertex}$	$(M\text{-}O\text{-}M)_{edge}$
HPMo[18]	1059	962	877	744
NaPCoMo	1049	946	869	772, 707
NaPNiMo	1047	942	869	783
nBu_4NPCu_2Mo	1077, 1055	935	864	777
NaPZnMo	1075, 1060 1045	939	900	775
NaPFeMo	1051	945	864	766
$NaPIn_3Mo$	1058	956	867	770
NaKPNbMo	1058, 1034	944	859	741
$NaKPNb_2Mo$	1049	947	856	757
$NaKPNb_3Mo$	1047	944	857	760
$NaKPV_2NbMo$	1045	942	847	750
$NaKPVNb_2Mo$	1048	944	859	762
$NaPV_3Mo$	1064, 1048	937	846	758
$NaPW_3Mo$	1058	964	909, 865	799

2.2 NMR spectroscopy

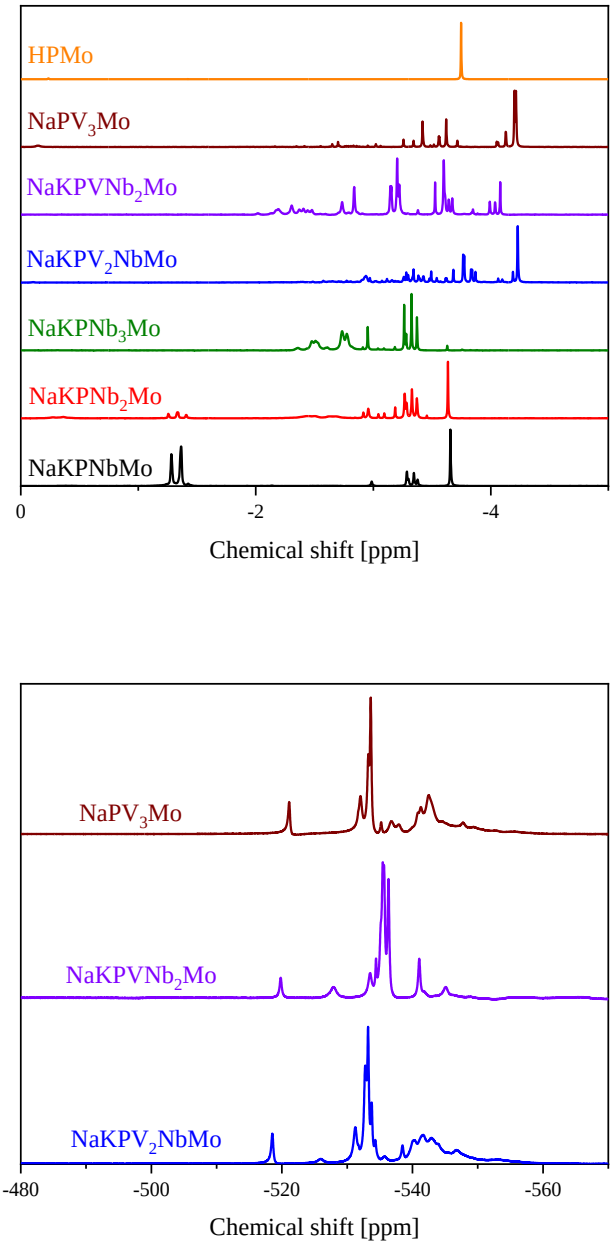

Figure S21: ^{31}P-NMR (top) and ^{51}V-NMR spectra (bottom) of the with pentavalent elements substituted POMs in a mixture of 90 % H2O (pH 1) and 10 % D2O. The spectra were measured at 242.9 MHz (^{31}P) 157.8 MHz (^{51}V). A 85 % H_3PO_4 and $NaVO_3$ were used as external standards.

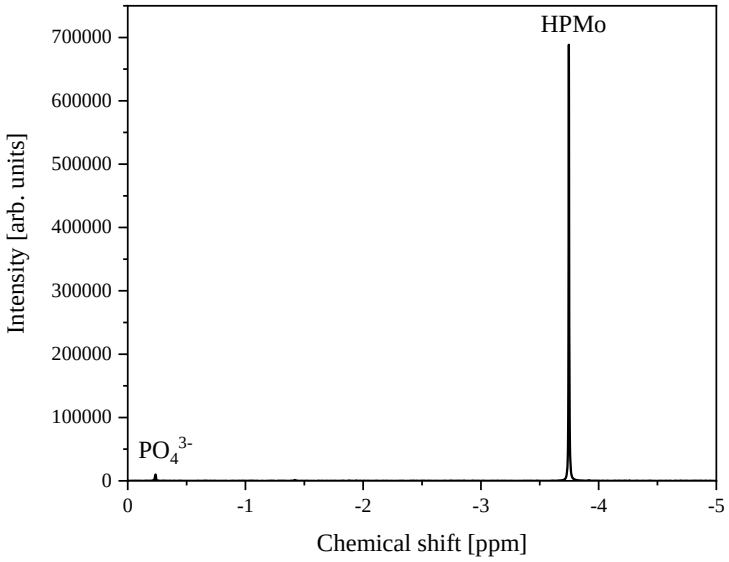

Figure S22: ^{31}P-NMR spectrum of HPMo in a mixture of 90 % H_2O (pH 1) and 10 % acetone-d6. The spectrum was measured at 242.9 MHz. 85 % H_3PO_4 was used as external standard.

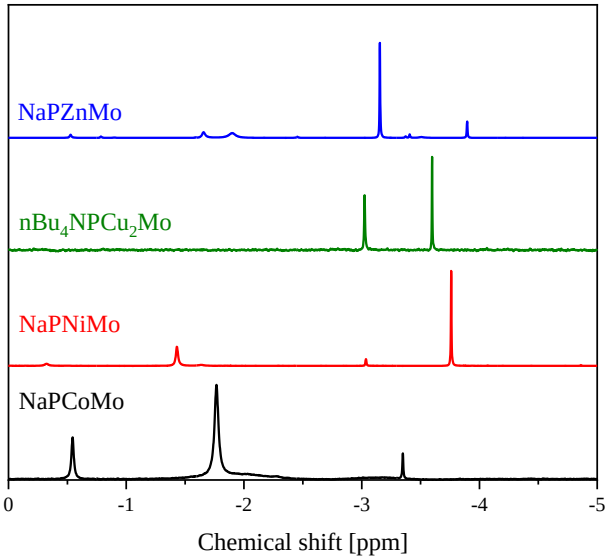

Figure S23: ^{31}P-NMR spectra of the with divalent elements substituted POMs in a mixture of 90 % H_2O (pH 1 10 % D_2O. The spectra were measured at 242.9 MHz. 85 % H_3PO_4 was used as external standard.

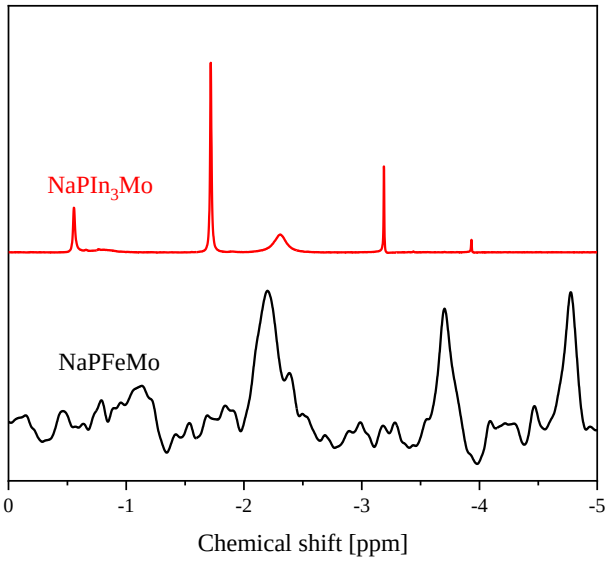

Figure S24: ^{31}P-NMR spectra of the with trivalent elements substituted POMs in a mixture of 90 % H_2O (pH 1 10 % D_2O. The spectra were measured at 242.9 MHz. 85 % H_3PO_4 was used as external standard.

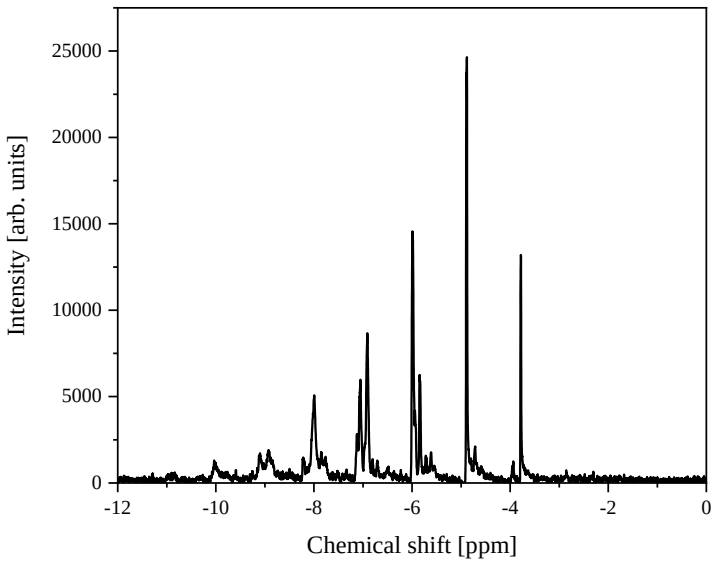

Figure S25: ^{31}P-NMR spectra of the with hexavalent elements substituted POMs in a mixture of 90 % H_2O (pH 1) and 10 % D_2O. The spectra were measured at 242.9 MHz. 85 % H_3PO_4 was used as external standard.

The ^{51}V NMR spectra of $NaPV_3Mo$, $NaKPVNb_2Mo$, and $NaKPV_2NbMo$ (Figure S21) show a fairly similar pattern of signals in the range of -510 ppm to -560 ppm, with each peak

representing an isomer or dissociation derivative of the respective compound. A broad peak at about -540 ppm indicates the presence of the VO_2^+ cation, [19] which may be formed through the above described dissociation. Additional NMR spectra of the POMs substituted with different elements are found in Figures S22-S25.

Table 6: Chemical shifts obtained from the ^{31}P and ^{51}V NMR spectra of the different compounds.

POM	^{31}P shift [ppm]	^{51}V shift [ppm]
HPMo	-3.75	-
NaPCoMo	-0.54, -1.77, -3.36	-
NaPNiMo	-3.76	-
nBu_4NPCu_2Mo	-3.02, -3.60	-
NaPZnMo	-0.53, -0.79, -1.59, -1.66, -1.90, -2.45, -3.15, -3.27, -3.41, -3.90	-
NaPFeMo	-	-
$NaPIn_3Mo$	-0.56, -1.72, -2.31, -3.19, -3.93	-
NaKPNbMo	-1.28, -1.37, -1.43, -2.99, -3.29, -3.30, -3.36, -3.38, -3.66	-
$NaKPNb_2Mo$	-0.28, -0.36, -1.26, -1.33, -1.40, -2.45, -2.51, -2.63, -2.92, -2.96, -3.04, -3.09, -3.19, -3.27, -3.28, -3.33, -3.37, -3.46, -2.64	-
$NaKPNb_3Mo$	-2.36, -2.48, -2.52, -2.61, -2.73, -2.78, -2.91, -2.96, -3.04, -3.09, -3.18, -3.26, -3.28, -3.33, -3.37, -3.63	-
$NaKPV_2NbMo$	-2.50 to -4.30	-517.7, -525.9, -531.3, -532.8, -533.2, -533.8, -534.3, -535.7, -538.5, -540 to -546
$NaKPVNb_2Mo$	-4.92, -5.08, -5.27 to -5.36, -5.49, -5.62, -5.69, -5.93, -5.96, -5.99, -6.04, -6.20, -6.30, -6.42, -6.43, -6.49, -6.54, -6.73, -6.77, -6.86, -6.88, -6.89, -6.90	-519.8, -527.9, -532.7, -533.7, -534.4, -535.4, -537.1, -545.1
$NaPV_3Mo$	-0.15, -2.70, -2.96, -3.02, -3.06, 3.26, -3.34, -3.42, -3.49, -3.52, -3.56, -3.62, -3.72, -4.05, -4.06, -4.13, -4.20, -4.21	-521.1, -532.0, -533.3, -533.6, -535.2, -536.8, -535.9, -540.8, -541.3, -542.9, -544.5, -547.8, -549.4
$NaPW_3Mo$	-1.63 to -12.45	-

2.3 UV-Vis spectroscopy

Additional UV-Vis spectra of the POMs substituted with different elements are found in Figures S26-S29:

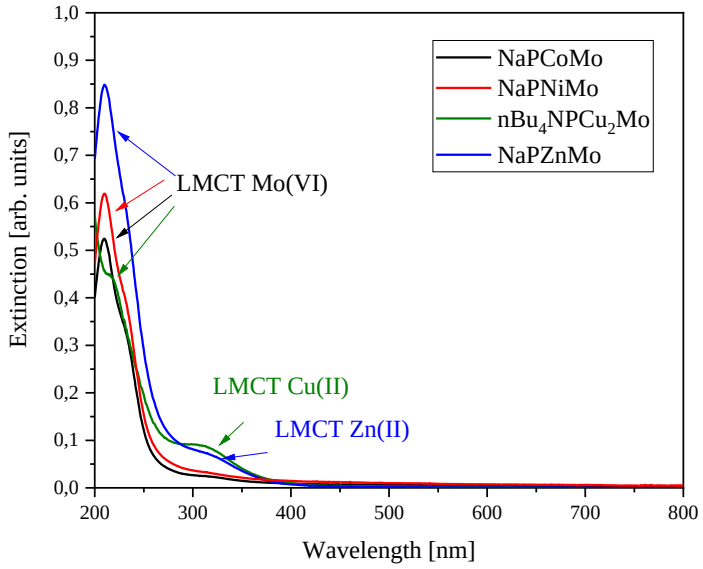

Figure S26: UV-Vis spectra of the with divalent elements substituted POMs in water.

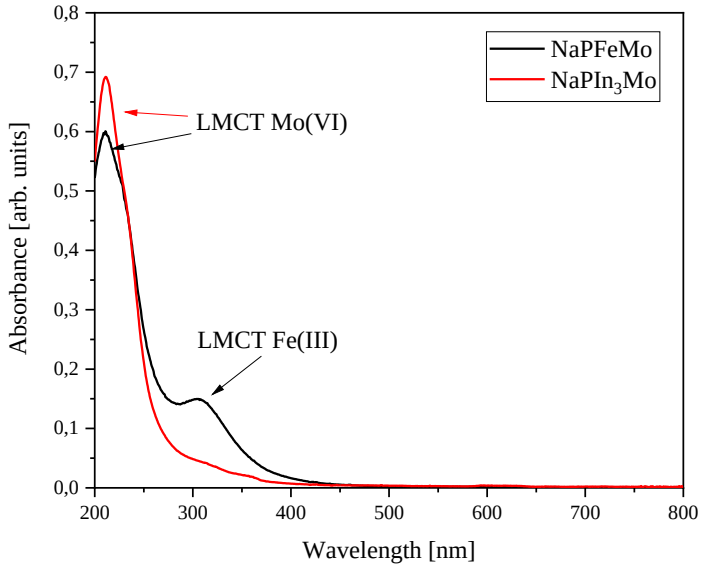

Figure S27: UV-Vis spectra of the with trivalent elements substituted POMs in water.

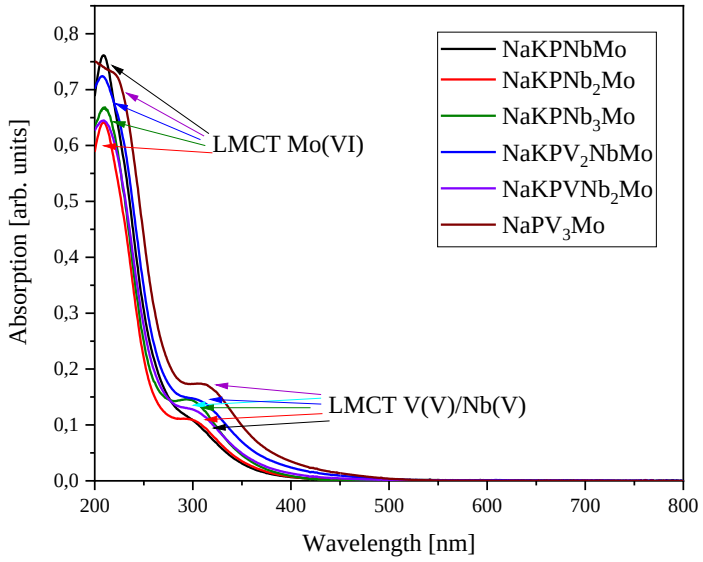

Figure S28: UV-Vis spectra of the with pentavalent elements substituted POMs in water.

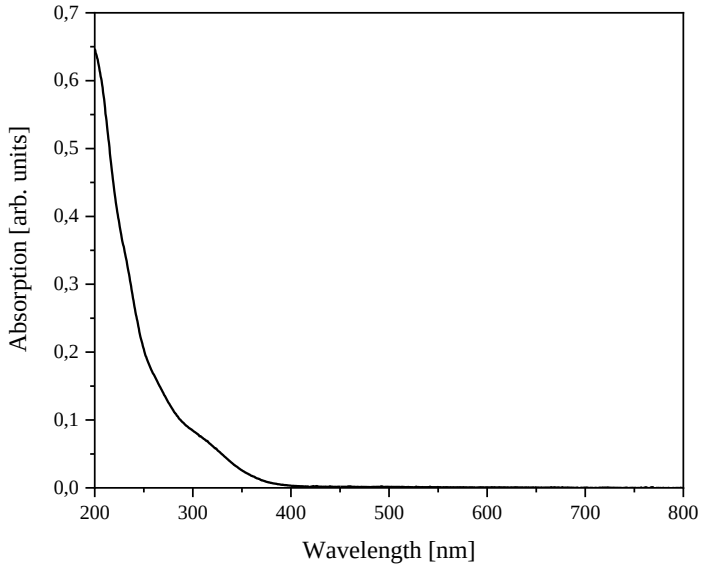

Figure S29: UV-Vis spectra of the with hexavalent elements substituted POMs in water.

Table 7: LMCT positions of the different POMs measured using UV-Vis spectroscopy.

POM/LMCT [nm]	Mo(VI)	W(VI)	Cu(II)	Zn(II)	Fe(III)	V(V)	Nb(V)
HPMo	218	-	-	-	-	-	-
NaPCoMo	210	-	-	-	-	-	-
NaPNiMo	210	-	-	-	-	-	-
nBu_4NPCu_2Mo	214	-	306	-	-	-	-
NaPZnMo	210	-	-	311	-	-	-
NaPFeMo	211	-	-	-	305	-	-
$NaPIn_3Mo$	211	-	-	-	-	-	-
NaKPNbMo	209	-	-	-	-	-	301
$NaKPNb_2Mo$	209	-	-	-	-	-	292
$NaKPNb_3Mo$	210	-	-	-	-	-	292
$NaKPV_2NbMo$	208	-	-	-	-	300	
$NaKPVNb_2Mo$	209	-	-	-	-	297	
$NaKPV_3Mo$	214	-	-	-	-	308	
$NaKPW_3Mo$	299		-	-	-	-	-

2.4 Electrochemistry

2.4.1 Electrochemical characterization of LHPA-3

In order to complete the characterisation of LHPA-3 and provide a solid analytical basis for the characterisation of transition metal substituted POMs, LHPA-3 was also studied with electrochemical methods, specifically CV and SWV (Figure S30 and S31).

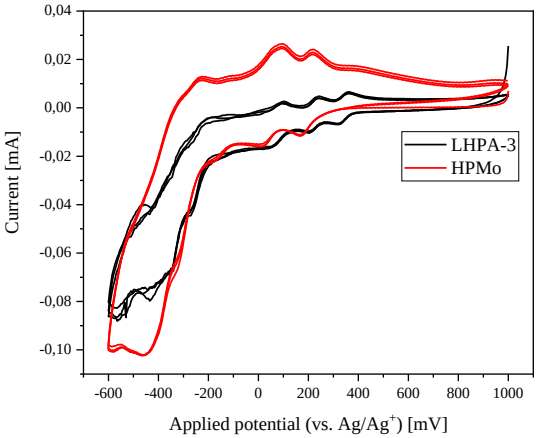

Figure S30: CV measurements of LHPA-3 and HPMo (concentration 1 mmol/L, scan rate 100 mV/s and pH 1). Hydrochloric acid was used as supporting electrolyte.

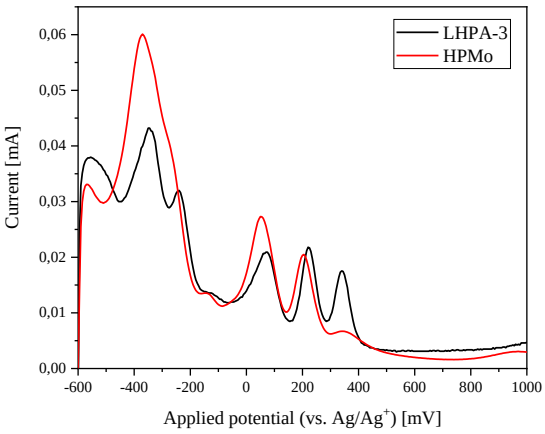

Figure S31: SWV measurements of LHPA-3 and HPMo (concentration 1 mmol/L, scan rate 5 mV/s and pH 1). Hydrochloric acid was used as supporting electrolyte.

Table 8 lists the electrochemical potentials identified in these electrochemical investigations. In comparison to HPMo, the Redox potentials of LHPA-3 are shifted to higher voltages. The SWV voltammogram shows an additional peak for LHPA-3 in the range of -600 to -200 mV, which is not resolved for HPMo, although the peak at -370 mV appears asymmetric with a shoulder on its right side. This indicates that the peak is caused by two overlapping signals.

Table 8: Electrochemical potentials of LHPA-3 and HPMo as determined by CV and SWV.

Redox process [a]	**CV potential** [b] **[mV]**	**SWV potential** [c] **[mV]**
LHPA-3		
	-	-555
	-	-350
	-	-240
$[PMo^{VI}_{9}O_{34}]]^{9-}$ / $[PMo^{VI}_{8}Mo^{IV}O_{34}]]^{11-}$	80	70

$[PMo^{VI}_{8}Mo^{IV}_{1}O40]]^{11-}$ / $[PMo^{VI}_{7}Mo^{IV}_{2}O40]]^{13-}$	223	220
	340	340
HPMo		
	-	-570
	-	-370
	-198	-150
$[PMo^{VI}_{12}O_{40}]]^{3-}$ / $[PMo^{VI}_{11}Mo^{IV}O_{40}]]^{5-}$	-39.7	50
$[PMo^{VI}_{11}Mo^{IV}O_{40}]]^{5-}$ / $[PMo^{VI}_{10}Mo^{IV}_{2}O40]]^{7-}$	193	205
	-	340

[a)] assignment based on literature values [20,21], [b)] mean value between oxidation and reduction pathway, [c)] peak maximum

This leads to the fundamental conclusion, that LHPA-3 and HPMo undergo similar Redox processes. However, the structural changes cause a shift in the respective potentials. The cyclovoltammograms indicate that the observed Redox processes are reversible, which makes LHPA-3 a suitable basis for the development of Redox catalysts.

Table 9: Peak maxima from SWV data, peak maxima (oxidation pathway) and peak minima (reduction pathway) from the CV data of LHPA-3 in comparison with HPMo in solution (solvent water) at pH 1 (HCl): concentration 1 mmol/L: scan rate 100 mV/s (CV) and 5 mV/s (SWV).

Maximum oxidation pathway (CV) [mV]	**Minimum reduction pathway (CV) [mV]**	**Mean value (CV) [mV]**	**Maximum SWV [mV]**	**Redox process**[20,21]
LHPA-3				
-	-	-	-555	-
-	-	-	-350	-
-	-	-	-240	-
100	60	80	70	$[PMo^{VI}_{8}Mo^{IV}O_{34}]^{11-}$
240	205	223	220	$[PMo^{VI}_{7}Mo^{IV}_{2}O_{40}]^{13-}$
360	320	340	340	-
HPMo				
-	-	-	-570	-
-	-	-	-370	-
-227	-169	-198	-150	.
-87.7	8.33	-39.7	50	$[PMo^{VI}_{11}Mo^{IV}O_{40}]^{5-}$
218	167	193	205	$[PMo^{VI}_{10}Mo^{IV}_{2}O_{40}]^{7-}$
-	-	-	340	-

2.4.2 Electrochemical characterization of the transition metal substituted POMs

Additional CV and SWV data of the POMs substituted with different elements are found in Figures S32-S39:

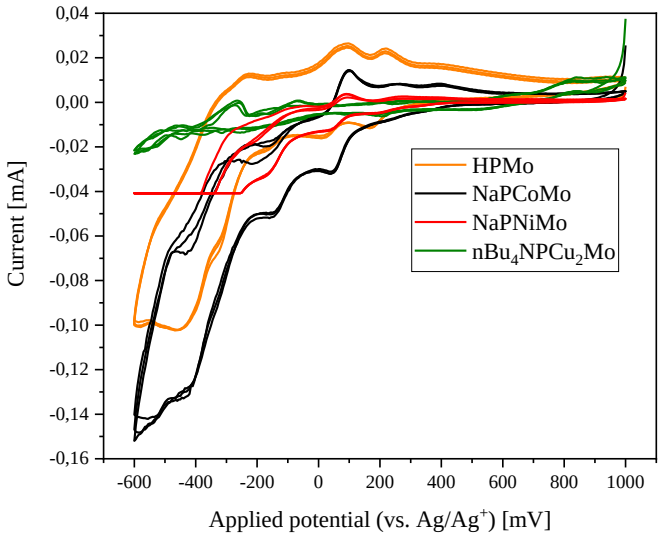

Figure S32: Comparison between the CV measurements of the with divalent elements substituted POMs in comparison with HPMo (concentration 1 mmol/L, scan rate 100 mV/s (CV) and pH 1). Hydrochloric acid was used as supporting electrolyte. nBu_4NPCu_2Mo was measured in acetonitrile. Tetrabutylammonium hexafluorophosphate was used as supporting electrolyte.

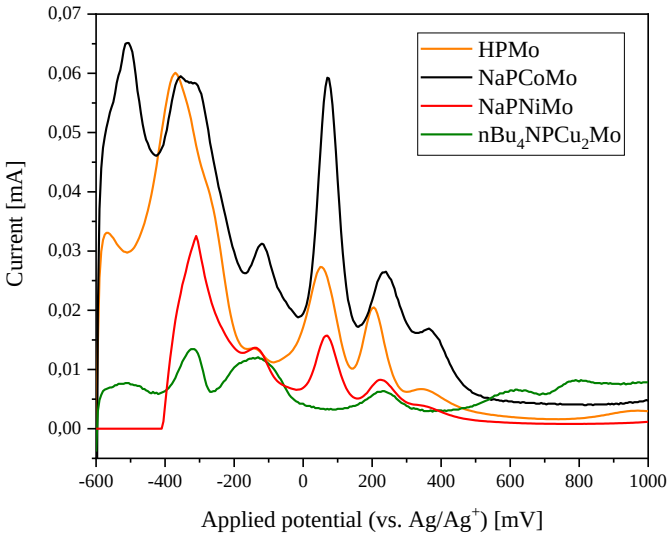

Figure S33: Comparison between the SWV measurements of the with divalent elements substituted POMs in comparison with HPMo (concentration 1 mmol/L, scan rate 5 mV/s (SWV) and pH 1). Hydrochloric acid was used as supporting electrolyte. nBu_4NPCu_2Mo was measured in acetonitrile. Tetrabutylammonium hexafluorophosphate was used as supporting electrolyte.

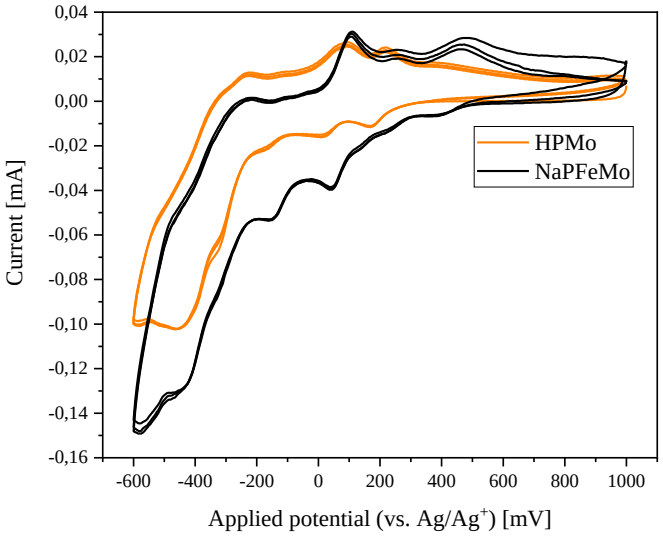

Figure S34: Comparison between the CV measurements of the with trivalent elements substituted POMs in comparison with HPMo (concentration 1 mmol/L, scan rate 100 mV/s (CV) and pH 1). Hydrochloric acid was used as supporting electrolyte.

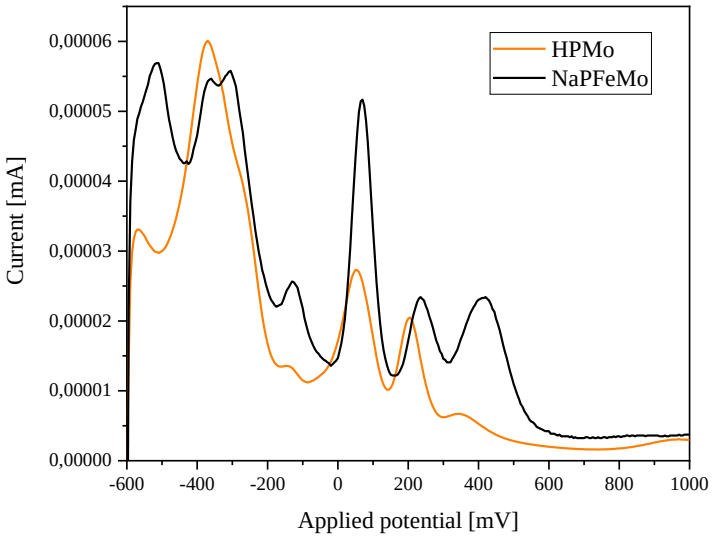

Figure S35: Comparison between the SWV measurements of the with trivalent elements substituted POMs in comparison with HPMo (concentration 1 mmol/L, scan rate 5 mV/s (SWV) and pH 1). Hydrochloric acid was used as supporting electrolyte.

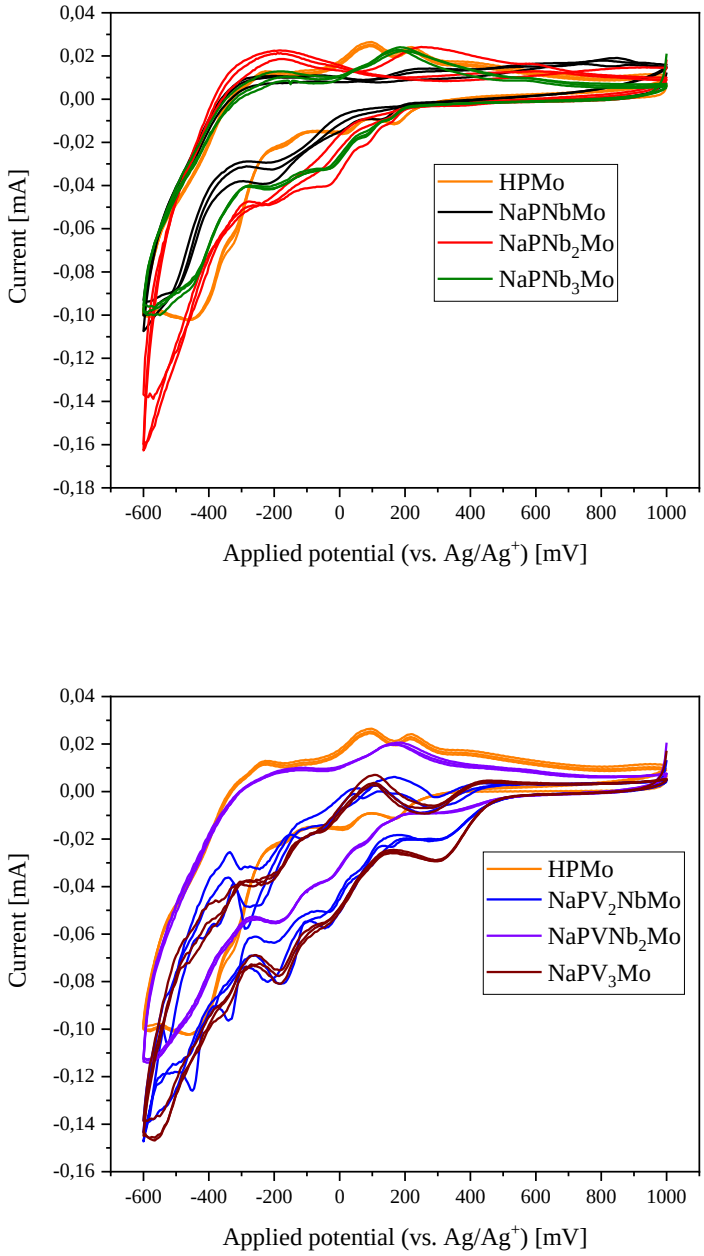

Figure S36: Comparison between the CV measurements of the with pentavalent elements substituted POMs in comparison with HPMo (concentration 1 mmol/L, scan rate 100 mV/s (CV) and pH 1). Hydrochloric acid was used as supporting electrolyte.

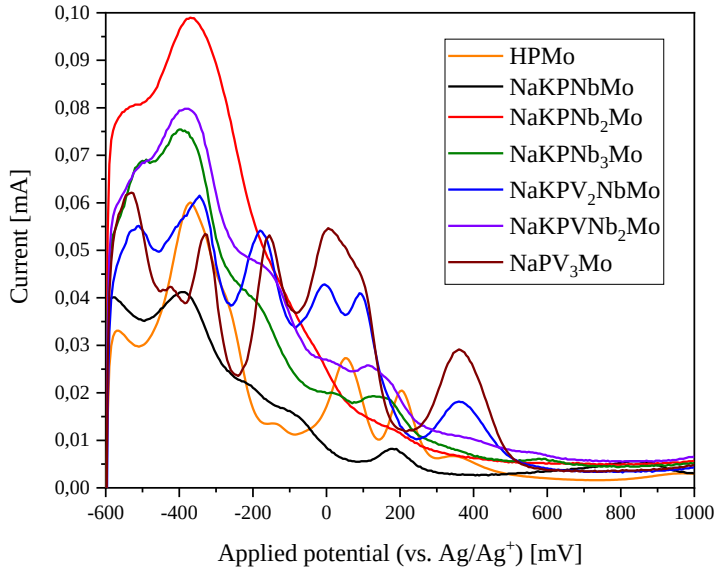

Figure S37: Comparison between the SWV measurements of the with pentavalent elements substituted POMs in comparison with HPMo (concentration 1 mmol/L, scan rate 5 mV/s (SWV) and pH 1). Hydrochloric acid was used as supporting electrolyte.

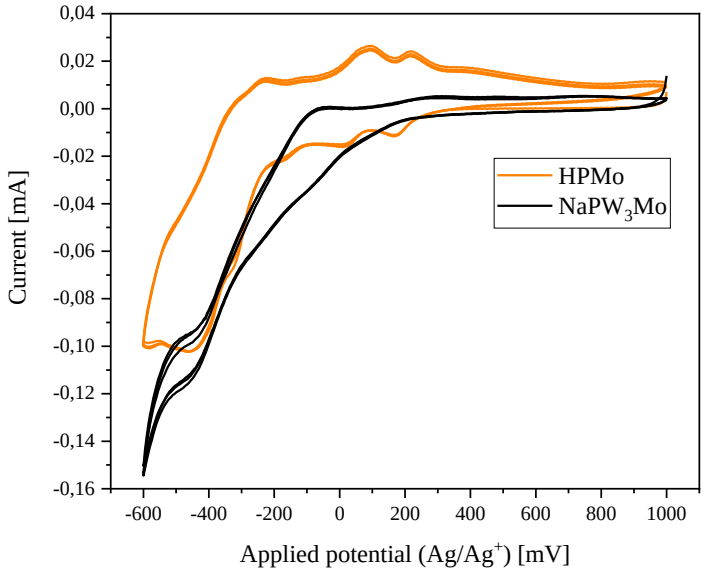

Figure S38: Comparison between the CV measurements of the with hexavalent elements substituted POMs in comparison with HPMo (concentration 1 mmol/L, scan rate 100 mV/s (CV) and pH 1). Hydrochloric acid was used as supporting electrolyte.

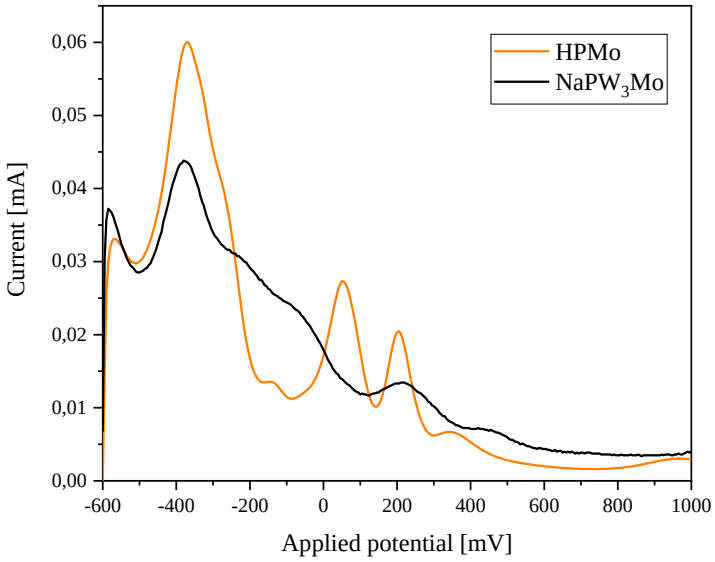

Figure S39: Comparison between the SWV measurements of the with hexavalent elements substituted POMs in comparison with HPMo (concentration 1 mmol/L, scan rate 5 mV/s (SWV) and pH 1). Hydrochloric acid was used as supporting electrolyte.

Table 10: Peak maxima from SWV data, peak maxima (oxidation pathway) and peak minima (reduction pathway) from the CV data of the POMs in solution (solvent water; acetonitrile for nBu_4NPCu_2Mo) at pH 1 (HCl): concentration 1 mmol/L: scan rate 100 mV/s (CV) and 5 mV/s (SWV).

Maximum oxidation pathway (CV) [mV]	Minimum reduction pathway (CV) [mV]	Mean value (CV) [mV]	Maximum SWV [mV]	Redox process[20,21]
HPMo				
-	-	-	-570	-
-	-	-	-370	-
-227	-169	-198	-150	.-
-87.7	8.33	-39.7	50	$[PMo^{VI}_{11}Mo^{IV}O_{40}]^{5-}$
218	167	193	205	$[PMo^{VI}_{10}Mo^{IV}_{2}O40]^{7-}$
-	-	-	340	-
NaPCoMo				
-465	-440	-453	-510	-
-	-	-	-355	-
-300	-	-	-315	-
-225	-155	-190	-120	-
-60	-	-	-	-
100	35	78	70	$[PCoMo^{VI}_{10}Mo^{IV}O_{40}]^{9-}$
265	-	-	240	$[PCoMo^{VI}_{9}Mo^{IV}_{2}O_{40}]^{11-}$
390	-	-	360	-
NaPNiMo				

	-	-	-310	
-50	-	-	-135	
90	35	63	65	$[PNiMo^{VI}_{10}Mo^{IV}O_{40}]^{9-}$
270	185	228	225	$[PNiMo^{VI}_{9}Mo^{IV}_{2}O_{40}]^{11-}$
385	-	-	334	
nBu_4NPCu_2Mo				
			-525	-
-460	-450	-455		-
			-325	-
-265	-255	-260		-
-70	-	-	-135	-
200	-	-	230	$[PCu_2Mo^{VI}_{8}Mo^{IV}_{2}O_{40}]^{15-}$
640	-	-	615	-
840	-	-	790	-
NaPFeMo				
-475	-440	-458	-515	-
			-365	-
			-305	-
-230	-155	-193	-	-
110	40	75	70	$[PFeMo^{VI}_{10}Mo^{IV}O_{40}]^{8-}$
260	225	243	235	$[PFeMo^{VI}_{9}Mo^{IV}_{2}O40]^{10-}$
475	380	428	420	-
NaKPNbMo				
-515	-520	-518	-580	-
			-395	-
-245	-230	-238	-225	-
-	-	-	-105	-
-60	-	-	-	-
230	120	178	175	$[PNbMo^{VI}_{9}Mo^{IV}_{2}O40]^{8-}$
620	-	-	-	-
845	-	-	840	-
$NaKPNb_2Mo$				
-	-	-	-545	-
-	-	-	-370	-
-185	-215	-200	-	-
-	-35	-	-	-
-	70	-	-	$[PNb_2Mo^{VI}_{9}Mo^{IV}O_{40}]^{7-}$
-	140	-	150	$[PNb_2Mo^{VI}_{8}Mo^{IV}_{2}O40]^{9-}$
250	-	-	-	-
$NaKPNb_3Mo$				
-	-	-	-580	-
-455	-460	-458	-500	-
-	-	-	-400	-
-190	-215	-203	-220	-
-	-40	-	-	-
-	80	-	10	$[PNb_3Mo^{VI}_{8}Mo^{IV}O_{40}]^{8-}$
180	140	160	125	$[PNb_3Mo^{VI}_{7}Mo^{IV}_{2}O40]^{10-}$
-	-	-	155	-
555	-	-	575	-

$NaKPV_2NbMo$				
-545	-	-	-515	-
-	-450	-	-	-
-335	-340	-338	-345	-
-145	-175	-160	-180	-
-	-45	-	-10	-
40	-	-	90	$[PV_2NbMo^{VI}_8Mo^{IV}O_{40}]^{8-}$
105	-	-	-	$[PV_2NbMo^{VI}_7Mo^{IV}_2O40]^{10-}$
170	145	158	-	-
-	230	-	-	-
-	-	-	360	-
430	-	-	-	-
$NaKPVNb_2Mo$				
-	-	-	-570	-
-	-	-	-505	-
-	-	-	-385	-
-165	-210	-188	-195	-
-	-55	-	-	-
-	65	-	10	$[PVNb_2Mo^{VI}_8Mo^{IV}O_{40}]^{8-}$
160	-	-	115	$[PVNb_2Mo^{VI}_7Mo^{IV}_2O40]^{10-}$
-	305	-	-	-
$NaPV_3Mo$				
-485	-	-	-530	-
-380	-	-	-425	-
-305	-	-	-	-
-300	-355	-328	-330	-
-115	-185	-150	-155	-
-	-35	-	5	$[PV_3Mo^{VI}_8Mo^{IV}O_{40}]^{8-}$
90	-	-	-	$[PV_3Mo^{VI}_7Mo^{IV}_2O40]^{10-}$
430	305	368	360	-
$NaPW_3Mo$				
-	-	-	-585	-
-490	-460	-475	-	-
-	-	-	-380	-
-	-	-	-245	-
-70	-	-	-10	-
250	-	-	210	-
-	-	-	450	-

2.5 X-ray diffraction

Figure S40 and S41 show the asymmetric unit and the solid-state structure of LHPA-3:

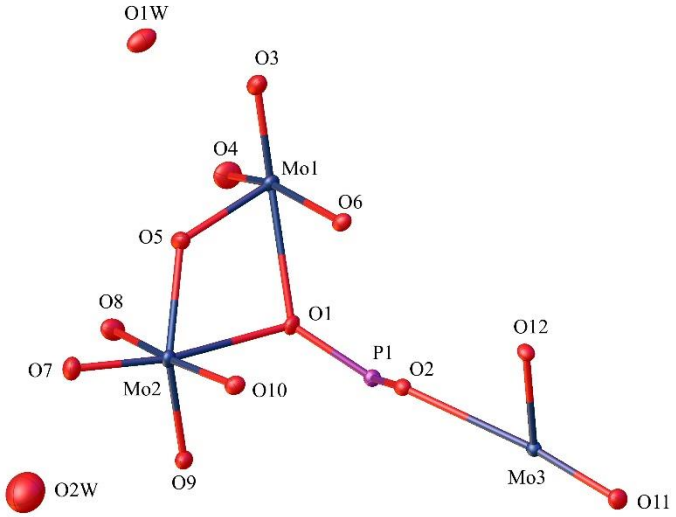

Figure S40: Asymmetric unit of the solid-state structure of LHPA-3 containing 18 atoms (one P, three Mo, twelve O of the POM structure and two additional O from crystal water molecules named OW).

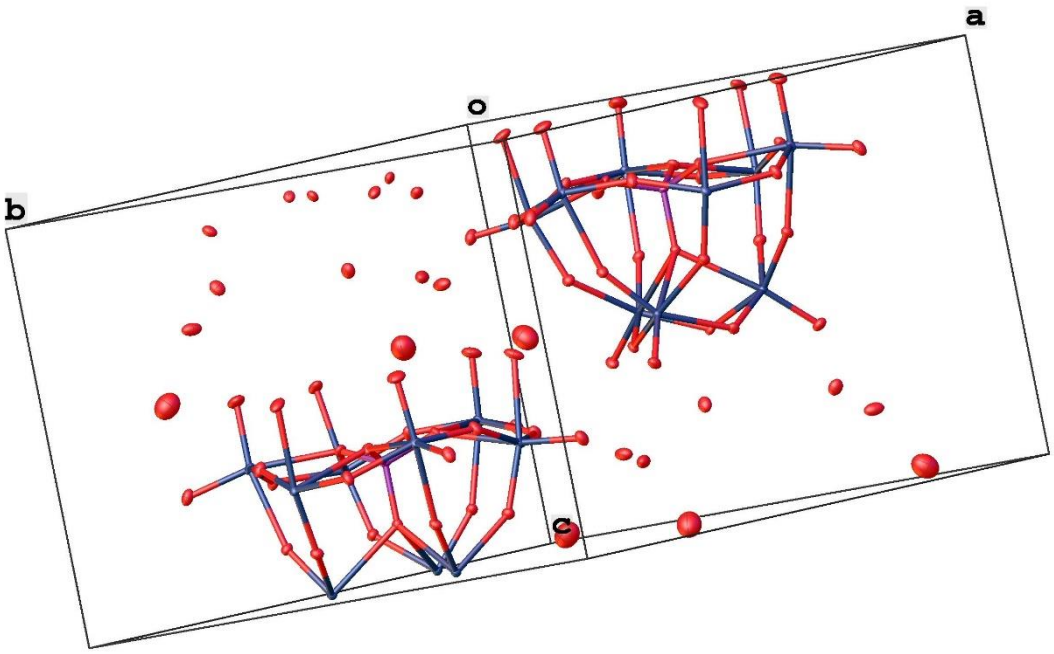

Figure S41: Unit cell of the solid-state structure of LHPA-3.

Table 11: Found bond lengths in LHPA-3 in comparison with sum of covalent radii.[22]

Bond	Average length [Å]	Sum of covalent radii [Å]
P - O_P	1.545	1.74
O_P - Mo	2.361	2.01
O_b - Mo	1.882	2.01
Mo - O_t	1.700	2.01
Mo - O_l	1.956	2.01

Furthermore, analogous to the species $[PW_9O_{34}]^{9-}$ already known[23] in the literature, a dimerization of LHPA-3 to a corresponding Wells-Dawson structure $[P_2Mo_{18}O_{62}]^{6-}$ was observed, which is thermally induced.[24] The presence of the dimerized species was confirmed by X-ray single crystal structure analysis, see Figure S42 and S43:

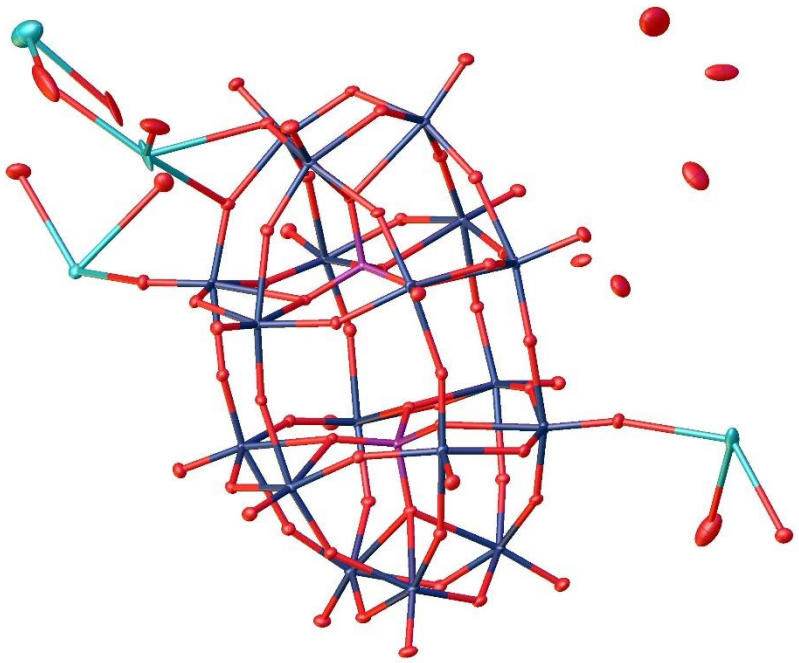

Figure S42: Solid-state structure and asymmetric unit of the dimerized LHPA-3 species as determined by single crystal X-ray diffraction. The compound crystallizes in the triclinic space group *P-1* (2). Hydrogen atoms have not been modeled. R_1: 3.11 %, wR_2: 7.93 %, R_{int}: 2.98 %, GooF: 1.029. Color code: purple: phosphorous, blue: molybdenum, red: oxygen and turquoise: alkali cations (sodium and potassium).

The LHPA-3 dimer shown in Figure S42 is a Wells-Dawson type structure in which the total 18 Mo atoms are in an octahedral coordination by six oxygen atoms. Each 9 Mo atoms originate from one LHPA-3 monomer. The structure is terminated by the presence of terminal oxygen atoms. Characteristic of a Wells-Dawson type structure are the two phosphorus heteroatoms, all in a tetrahedral coordination of four oxygen atoms, in the centre of the

structure, with one P atom each contributed by an LHPA-3 monomer. There are a total of four alkali cations in the asymmetric unit, with two cations refined as sodium (between O1W to O3W) and two others as potassium (O4W to O7W). The alkali metal counterions coordinate to the terminal oxygen atoms and are all in a distorted octahedral environment of six oxygen atoms, with two alkali metal ions bridged by two hydrate water molecules each. Hydrate water molecules are visualized by individual oxygen atoms in Figure 42, where the H atoms were not modeled due to the low scattering contribution in X-ray crystallography.

The compound was crystallized in the triclinic space group *P-1* (2) with lattice parameters of a = 12.7114(1) Å, b = 14.7642(2) Å, c = 19.7054(2) Å, α = 102.465(1) °, β = 99.119(1) °, and γ = 114.620(1) °. The crystallographic data are available as a .cif file in the CCDC database (deposition number: 2216946).

The average bond length of the P1,2-O1-4,26-29 bonds are 1.543 Å, while the average bond lengths of the O1-4,26-29-Mo1-18 bonds are 2.346 Å. Compared with the sum of the covalent radii[25] of a P-O (1.74 Å) and an O-Mo (2.01 Å) bond, it is noticeable that the P1,2-O1-4,26-29 bonds are shorter than the sum of the covalent radii and thus stronger in nature, while the O1-4,26-29-Mo1-18 bonds are significantly longer and thus have more coordinative character. The bond lengths of the oxygen-metal bridging bonds are approximately 1.943 Å, which is shorter than the bond distance calculated by the sum of the covalent radii (2.01 Å). Here, too, the terminal oxygen atoms with an average bond length of 1.689 Å show a significantly shortened distance due to the double bond character. The average distance of the alkali metal counterions was determined to be 2.698 Å, while the average distance of the alkali ions to the coordinated hydrate water molecules is 2.729 Å. Compared to the sum of the covalent radii, the calculated bond distance (K: 196 pm; O: 63 pm[25]) is 2.59 Å (259 pm) for a O-K bond and 2.18 Å (218 pm) for a O-Na bond (Na: 155 pm; O: 63 pm[25]). Since the values found are above the extrapolated value, the coordinative bonding nature of the POM/hydrated water alkali ion interaction is also evident here.

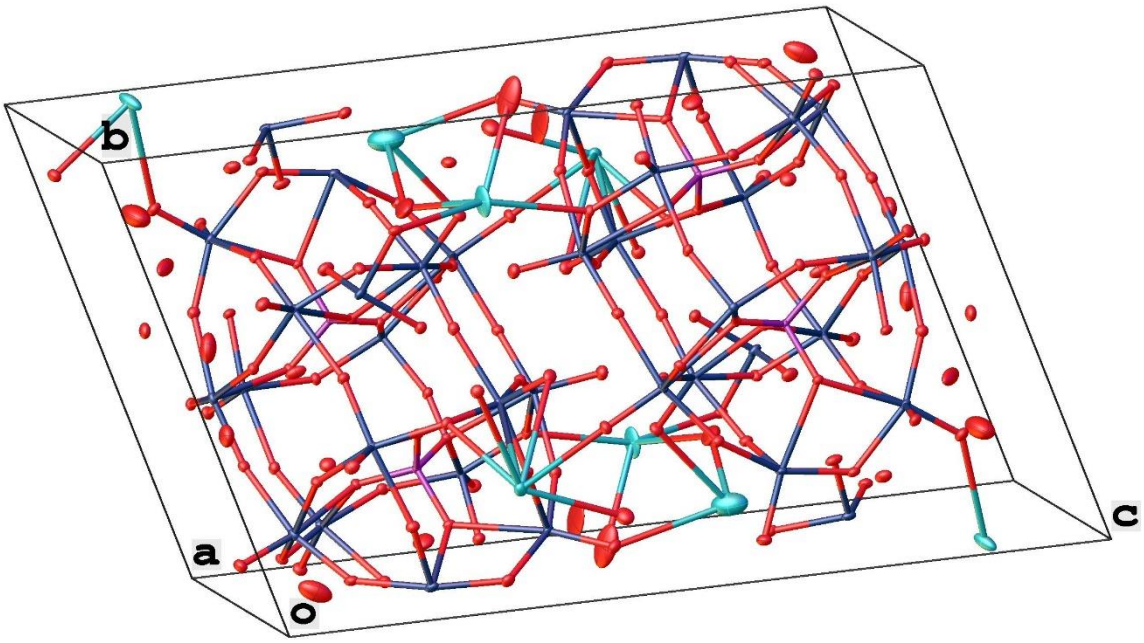

Figure S43: Unit cell of the solid-state structure of dimerized LHPA-3.

The solid-state structure of KNb is shown in Figure S44:

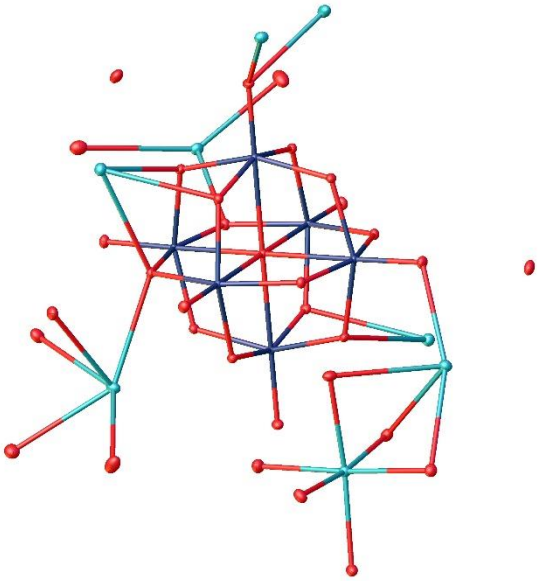

Figure S44: Solid-state structure and asymmetric unit of KNb determined by single crystal X-ray diffraction. The compound crystallizes in the monoclinic space group $P2_1/c$ (14). Hydrogen atoms have not been modeled. R_1: 2.58 %, wR_2: 6.73 %, R_{int}: 3.08 %, GooF: 1.252. Color code: turquoise: potassium/sodium, blue: niobium, and red: oxygen.

The compound was crystallized in the hexagonal space group $P2_1/c$ (14) with the lattice parameters a = 12.63957(11) Å, b = 10.69819(9) Å and c = 24.23416(18) Å and the lattice angles α = 90 °, β = 92.1646(7) ° and γ = 90 °. For the isopolyanion (IPA) there are six Nb(V) atoms in a distorted octahedral coordination geometry by six oxygen atoms. The central oxygen atom is in an octahedral coordination of the six Nb(V) atoms. Potassium atoms are in an octahedral environment of six oxygen atoms: the cations are coordinated by four oxygen atoms of hydration water molecules and by two terminal oxygen atoms. So, one potassium is connecting two IPAs. During the refinement process it was observed that the electron density for K1 is too high. One reason is that this position is in some unit cells occupied with an alkali ion of lower electron density such as sodium. This is likely due to the low purity of the potassium hydroxide used of 85 %. So, this position was refined using free variables with sodium and potassium. As a result, the occupancy for potassium was refined to be 0.87894 and for sodium to 0.12106. The sum of both is an occupancy of 1. A similar problem arose for K2: here, as the best result, it position was completely occupied and refined with sodium (occupancy of 1).

The average bond length of O1-Nb1-6 is 2.529 Å, the average bond length of the metal bridging bonds O2-13-Nb1-6 are 1.992 Å and the average length of the terminal oxygen metal bonds Nb1-6=O14-19 are 1.798 Å. Here, as expected, the bond length of Nb1-6=O14-19 is significant shorter than the sum of covalent radii[22] of 2.10 Å, due to the mentioned double bond character. It is also striking that the bond length of the central oxygen atom to the Nb(V) atoms O1-Nb1-6 is significant longer. This indicates the coordinative bond character as mentioned for the other crystal structures. The average distance between a terminal oxygen and an alkali cation was determined to be 2.760 Å. Furthermore, the average distance between hydration water molecules and alkali cations is 2.637 Å. So, those bond lengths are significant longer than the sum of covalent radii (see Table 12), indicating the coordinative bond character.

In comparison to Nb_2O_5 the bond lengths are about 1.65 Å to 1.68 Å.[26] Comparing to the sum of covalent radii of a Nb-O bond of 210 pm/2.10 Å (Nb: 147 pm, O: 63 pm[22]), the Nb-O bond in the oxide seems to be shorter, indicating covalent bond character. In the POM the Nb-O bond is than a little bit longer, but still shorter than the sum of covalent radii.[22,26]

Table 12 shows an comparison of the found bond lengths vs. the sum of covalent radii (Nb: 147 pm (1.47 Å) and O: 63 pm (0.63 Å)):[22]

Table 12: Found bond lengths in KNb in comparison with sum of covalent radii.[22]

Bond	Average length [Å]	Sum of covalent radii [Å]
O1-Nb1-6	2.529	2.10
O2-13-Nb1-6	1.992	2.10
Nb1-6=O14-19	1.798	2.10
O14-19-Na1,2/O14-19-K1,3-7	2.760	2.18/2.59
O1W-12W-Na1,2/O1W-12W-K1,3-7	2.637	2.18/2.59

Asymmetric unit of the solid-state structure of $NaPV_3Mo$ in Figure S45:

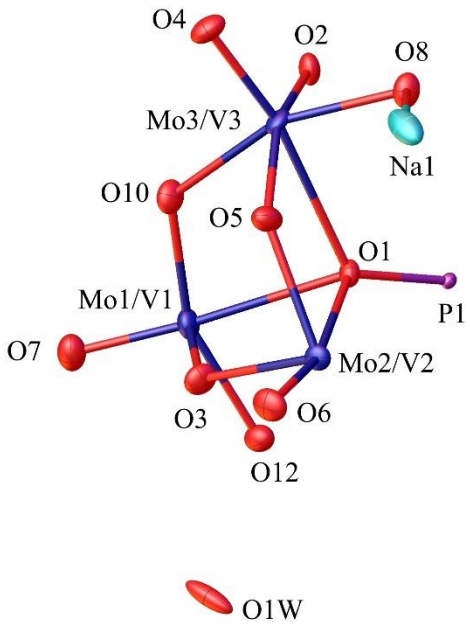

Figure S45: Asymmetric unit of the solid-state structure of $NaPV_3Mo$ containing 18 atoms (one P, three Mo/V, twelve O of the POM structure, an additional O from crystal water molecules named OW and a Na cation).

Table 13: Weighted average of calculated bond lengths (sum of covalent radii) and observed bond lengths of each bond in each POM.

Bond types	P1-O1	O1-M1-3	O2-7-M1-3	M1-3=O8-10
Sum of covalent radii* [Å]	1.74	2.00	2.00	2.00
Observed bond length [Å]	1.537	2.410	1.921	1.665

*$BL = \frac{a(r_O + r_{Mo}) + b(r_O + r_V)}{a + b}$ with BL the weighted average bond length, r_x the covalent radii of the corresponding elements x and a and b the weighting factors (e. g. for $NaPV_3Mo$: $a = 9$ and $b = 3$).

Table 14: Crystal structure data and structure refinement for compounds LHPA-3, LHPA-3 dimer, $NaPV_3Mo$ and KNb.

Compound	**LHPA-3**	**LHPA-3 dimer**	**$NaPV_3Mo$**	**KNb**
Empirical formula	$Mo_{18}O_{80}P_2$	$K_2Mo_{18}Na_2O_{74.96}P_2$	$Mo_9Na_4O_{42}PV_3$	$K_{6.91}Na_{1.09}Nb_6O_{33}$
Formula weight	3068.86	3112.40	1811.21	1380.74
Temperature/K	99.95(13)	99.95(16)	100.01	99.96(13)
Crystal system	hexagonal	triclinic	tetragonal	Monoclinic
Space group	*P6₃*	*P-1*	*P-42₁c*	*P21/c*
a [Å]	14.11802(9)	12.71140(10)	12.486(3)	2.63957(11)
b [Å]	14.11802(9)	14.7642(2)	12.486(3)	10.69819(9)
c [Å]	10.65823(8)	19.7054(2)	17.510(7)	24.26416(18)
α [°]	90	102.4650(10)	90	90
β [°]	90	99.1190(10)	90	92.1646(7)
γ [°]	120	114.6200(10)	90	90
Volume [$Å^3$]	1839.77(3)	3151.58(6)	2729.9(15)	3278.67(5)
Z	1	2	2	4
ρ_{calc} [g/cm^3]	2.770	3.280	2.203	2.797
μ [mm^{-1}]	3.121	3.781	2.626	3.030
F(000)	1426.0	2891.0	1684.0	2613.0
Crystal size [mm^3]	0.28 × 0.2 × 0.14	0.18 × 0.15 × 0.12	0.089 × 0.062 × 0.054	0.3 × 0.25 × 0.15
Radiation	Mo Kα (λ = 0.71073)	Mo Kα (λ = 0.71073)	MoKα (λ = 0.71073)	Mo Kα (λ = 0.71073)
2Θ range for data collection [°]	6.924 to 65.774	5.654 to 59.132	4.006 to 61.148	5.948 to 65.832
Index ranges	$-20 \le h \le 21$, $-20 \le k \le 21$, $-15 \le l \le 16$	$-17 \le h \le 17$, $-20 \le k \le 20$, $-27 \le l \le 27$	$-17 \le h \le 17$, $-17 \le k \le 17$, $-25 \le l \le 25$	$-19 \le h \le 18$, $-15 \le k \le 16$, $-36 \le l \le 36$
Reflections collected	118316	139713	140274	204566
Independent reflections	4488 [R_{int} = 0.0328, R_{sigma} = 0.0094]	16650 [R_{int} = 0.0298, R_{sigma} = 0.0162]	4184 [R_{int} = 0.0449, R_{sigm} = 0.0103]	11834 [R_{int} = 0.0308, R_{sigma} = 0.0112]
Data/restraints/parameters	4488/1/152	16650/0/886	4184/0/135	11834/0/425
Goodness-of-fit on F^2	1.111	0.829	1.089	1.252
Final *R* indexes [I>=2σ (I)]	R_1 = 0.0181, wR_2 = 0.0497	R_1 = 0.0311, wR_2 = 0.0800	R_1 = 0.0303, wR_2 = 0.0779	R_1 = 0.0258, wR_2 = 0.0670
Final *R* indexes [all data]	R_1 = 0.0182, wR_2 = 0.0498	R_1 = 0.0328, wR_2 = 0.0813	R_1 = 0.0308, wR_2 = 0.0784	R_1 = 0.0264, wR_2 = 0.0673
Largest diff. peak/hole [e $Å^{-3}$]	2.22/-0.68	6.56/-1.95	2.89/-0.65	2.49/-1.27
Deposition number	2205006	2216946	2205007	2216947

2.6 Microscopy

SEM images of the powder samples $NaKPNb_3Mo$ are shown in Figure S46-S48.

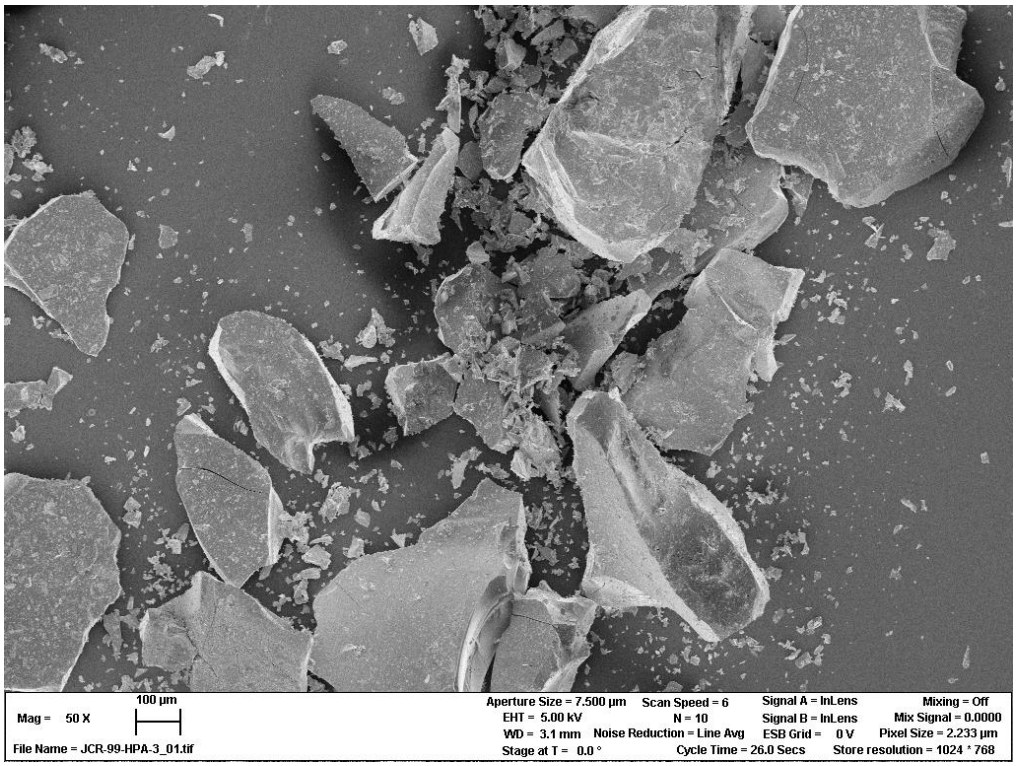

Figure S46: First SEM image of a selected area of a POM particle sample of $NaKPNb_3Mo$.

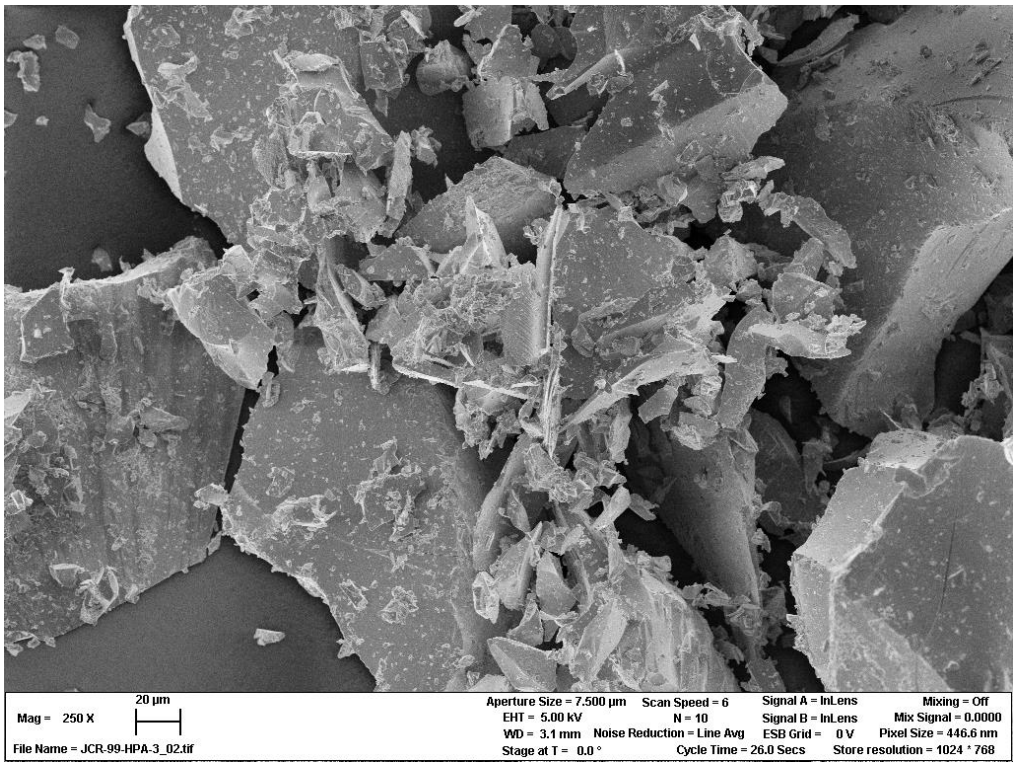

Figure S47: Second SEM image of a selected area of a POM particle sample of $NaKPNb_3Mo$.

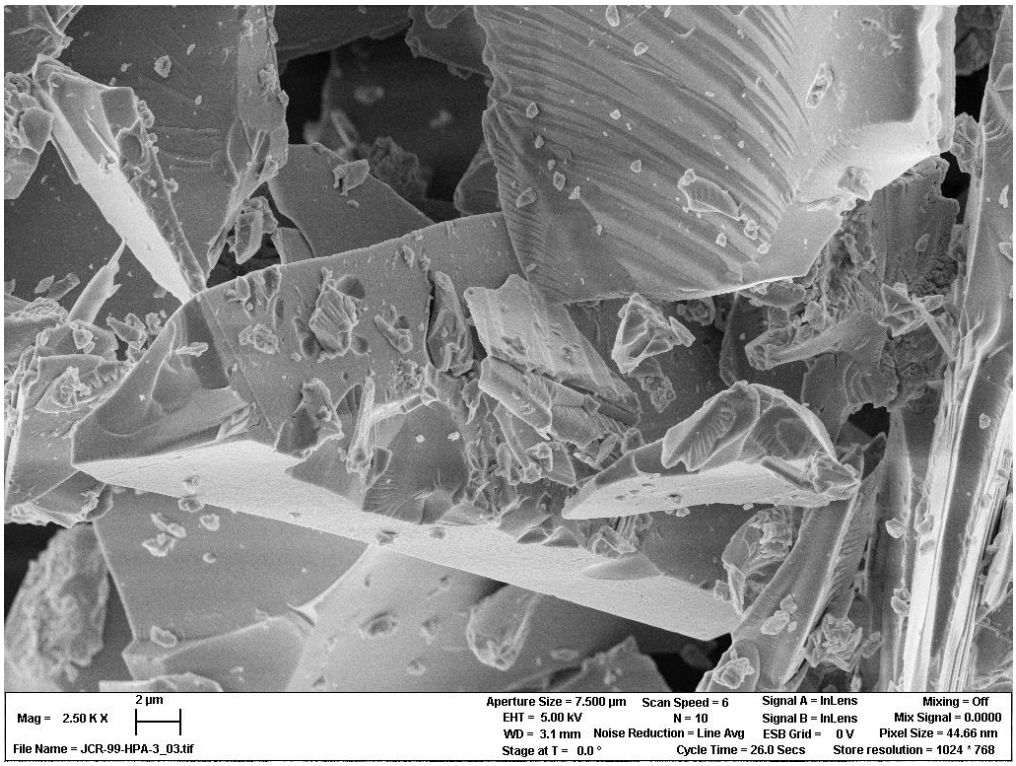

Figure S48: Third SEM image of a selected area of a POM particle sample of $NaKPNb_3Mo$.

Figure S49: Membrane plant used for nanofiltration to remove salts from the POM solution. Here: purification of $NaKPNb_3Mo$ (yellow solution).

3 Literature

1 A. L. Spek, Structure validation in chemical crystallography, *Acta Crystallogr. Sect. D Biol. Crystallogr.*, 2009, **65**, 148–155.

2 O. V. Dolomanov, L. J. Bourhis, R. J. Gildea, J. A. K. Howard and H. Puschmann, OLEX2: a complete structure solution, refinement and analysis program, *J. Appl. Crystallogr.*, 2009, **42**, 339–341.

3 G. M. Sheldrick, A short history of SHELX, *Acta Crystallogr. Sect. A Found. Crystallogr.*, 2008, **64**, 112–122.

4 C. B. Hübschle, G. M. Sheldrick and B. Dittrich, ShelXle: a Qt graphical user interface for SHELXL, *J. Appl. Crystallogr.*, 2011, **44**, 1281–1284.

5 A. L. Spek, Single-crystal structure validation with the program PLATON, *J. Appl. Crystallogr.*, 2003, **36**, 7–13.

6 T. Ressler, O. Timpe and F. Girgsdies, In situ bulk structural study on solid-state dynamics and catalytic activity correlations of a H4[PNbMo11O40] partial oxidation catalyst, *Zeitschrift fur Krist.*, 2005, **220**, 295–305.

7 M. Nyman, T. M. Alam, F. Bonhomme, M. A. Rodriguez, C. S. Frazer and M. E. Welk, Solid-state structures and solution behavior of alkali salts of the [Nb6O19]8- Lindqvist ion, *J. Clust. Sci.*, 2006, **17**, 197–219.

8 Y. C. Li, G. Lee, T. Yuan, Y. Wang, D.-H. Nam, Z. Wang, F. P. Garciá De Arquer, Y. Lum, C.-T. Dinh, O. Voznyy and E. H. Sargent, CO2 Electroreduction from Carbonate Electrolyte, *ACS Energy Lett.*, 2019, **4**, 1427–1431.

9 M. Tatzber, M. Stemmer, H. Spiegel, C. Katzlberger, G. Haberhauer and M. H. Gerzabek, An alternative method to measure carbonate in soils by FT-IR spectroscopy, *Environ. Chem. Lett.*, 2007, **5**, 9–12.

10 R. Mattes, H. Bierbüsse and J. Fuchs, Schwingungsspektren und Kraftkonstanten von Polyanionen mit M6O19-Gruppen, *Zeitschrift für Anorg. und Allg. Chemie*, 1971, **385**, 230–242.

11 P. Müscher-Polzin, C. Näther and W. Bensch, Hexaniobate anions connected by [Ni(cyclam)]2+ complexes yield two interpenetrating three- dimensional networks, *Zeitschrift für Naturforsch.*, 2020, **75**, 583–588.

12 V. Tsirelson and A. Stash, Orbital-free quantum crystallography: view on forces in crystals, *Acta Crystallogr. Sect. B Struct. Sci. Cryst. Eng. Mater.*, 2020, **76**, 769–778.

13 V. L. Cherginets, V. N. Baumer, S. S. Galkin, L. V. Glushkova, T. P. Rebrova and Z. V. Shtitelman, Solubility of Al2O3 in Some Chloride−Fluoride Melts, *Inorg. Chem.*, 2006, **45**, 7367–7371.

14 TURBOMOLE, V7.5.1 2021, a development of University of Karlsruhe and Forschungszentrum Karlsruhe GmbH, 1989–2007, TURBOMOLE GmbH, since 2007; available from http://www.turbomole.com.

15 M. Ernzerhof and G. E. Scuseria, Assessment of the Perdew–Burke–Ernzerhof exchange-correlation functional, *J. Chem. Phys.*, 1999, **110**, 5029–5036.

16 A. Schäfer, H. Horn and R. Ahlrichs, Fully optimized contracted Gaussian basis sets for atoms Li to Kr, *J. Chem. Phys.*, 1992, **97**, 2571–2577.

17 A. Klamt and G. Schüürmann, COSMO: a new approach to dielectric screening in solvents with explicit expressions for the screening energy and its gradient, *J. Chem. Soc., Perkin Trans. 2*, 1993, 799–805.

18 J.-C. Raabe, J. Albert and M. J. Poller, Spectroscopic, Crystallographic, and Electrochemical Study of Different Manganese(II)-Substituted Keggin-Type Phosphomolybdates, *Chem. – A Eur. J.*, 2022, **28**, 1–12.

19 C. Slebodnick and V. L. Pecoraro, Solvent effects on 51V NMR chemical shifts: characterization of vanadate and peroxovanadate complexes in mixed water/acetonitrile solvent, *Inorganica Chim. Acta*, 1998, **283**, 37–43.

20 D. Y. Hwang, Y. S. Ha and S. Kim, Electrode-Assisted Wacker Process: Phosphomolybdate-Mediated Oxidation of 1-Butene to Methyl Ethyl Ketone, *Bull. Korean Chem. Soc.*, 2001, **22**, 441–442.

21 M. Sadakane and E. Steckhan, Electrochemical Properties of Polyoxometalates as

Electrocatalysts, *Chem. Rev.*, 1998, **98**, 219–237.

22 P. Pyykkö and M. Atsumi, Molecular single-bond covalent radii for elements 1-118, *Chem. - A Eur. J.*, 2009, **15**, 186–197.

23 P. J. Domaille and G. Watunya, Synthesis and tungsten-183 NMR characterization of vanadium-substituted polyoxometalates based on B-type tungstophosphate PW9O349- precursors, *Inorg. Chem.*, 1986, **25**, 1239–1242.

24 C. Marchal-Roch, E. Ayrault, L. Lisnard, J. Marrot, F.-X. Liu and F. Sécheresse, Dimerization in Acetonitrile of [H6PMo9O34]3− into [P2Mo18O62]6−: Structural Characterization of the Tetrabutyl Ammonium Salt, *J. Clust. Sci.*, 2006, **17**, 283–290.

25 P. Pyykkö and M. Atsumi, Molecular Single-Bond Covalent Radii for Elements 1-118, *Chem. - A Eur. J.*, 2009, **15**, 186–197.

26 F. D. Hardcastle and I. E. Wachs, Determination of niobium-oxygen bond distances and bond orders by Raman spectroscopy, *Solid State Ionics*, 1991, **45**, 201–213.